Pre-Clinical Feasibility Assessment Of Pulmonary Delivery Of The Drug Risperidone For The Treatment Of Schizophrenia Using Jet Nebulizers And Electronic Cigarettes

A Thesis Submitted by

Sarah Armstrong

in partial fulfillment of the requirements for the degree of

Master of Science
in
Biomedical Engineering

Tufts University

May 2018

Thesis Committee

Dr. Anthony Barry
Dr. Mark Cronin-Golomb
Dr. David Kaplan

ABSTRACT

Schizophrenia possess a significant health burden and high rates of treatment non-adherence results in increased relapse rates, more frequent hospitalizations, higher levels of treatment-refractory residual symptoms and poorer long-term functioning and overall outcomes. Exploration of familiar routes of drug delivery that capitalize on existing habitual behaviors common in people with schizophrenia may offer a unique approach to improving treatment adherence in this population. For example, given the high prevalence of nicotine dependence in this population (78-88% schizophrenia vs 22.5% general population), individuals with schizophrenia might be more amenable to taking their medications via inhalation compared to the current standard of oral administration.

These studies demonstrate the technical feasibility of administering a clinically-relevant therapeutic dose of Risperidone via a jet nebulizer and an electronic-cigarettes, opening new avenues to increase and potentially monitor adherence and improve clinical outcomes.

ACKNOWLEDGEMENTS

I would like to thank everyone who, in various ways, supported me. I cannot verbalize the depth of my gratitude nor can the extent of their support be appropriately expressed or contained within this document's section.

I'm deeply indebted to Dr. Anthony Barry for giving me this unique and rich learning opportunity - I wouldn't have been able to explore this project without your guidance, support, and knowledge. I really enjoyed learning from you and I thank-you for this gift.

Thank-you Dr. David Kaplan and Dr. Cronin-Golomb for your involvement and participation in this process and playing a vital role as my committee members. completion. The depth of my gratitude for what you've given me, far exceeds what can be expressed in words.

TABLE OF CONTENTS

LIST OF TABLES

LIST OF FIGURES

OVERVIEW

The overall cost of schizophrenia in the United States as of 2002 was estimated to be $62.7 billion, of which at least $22.7 billion was related to direct health care expenses (3). Long--term hospitalization, homelessness, joblessness, comorbid medical and psychiatric illness, substantial functional impairment, disability support and early death are all associated with schizophrenia (4, 5). The public health burden is significant, and little progress has been made in the development of new antipsychotic medications since their introduction in the 1950s. The side effect profile of antipsychotic treatments—as well as high rates of treatment non-adherence due to functional impairment from the disease, and other factors—is a barrier to improved clinical outcome for many individuals with schizophrenia. Improvements in drug delivery and effectiveness have the potential to impact positively the public health and economic burden associated with the illness significantly, particularly given the relative dearth of novel agents or delivery mechanisms for schizophrenia in recent years. Exploration of familiar routes of drug delivery that capitalize on existing habitual behaviors common in people with schizophrenia may offer a unique approach to improving treatment adherence in this population (5). For example, given the high prevalence of nicotine dependence in this population (78-88% in schizophrenia vs 22.5% the general population (6)), individuals with schizophrenia might be more amenable to taking their medications via inhalation compared to the current standard of oral administration.

In this project, the technical feasibility of therapeutically delivering an antipsychotic medication by inhalation was explored and assessed through modeling, formulating, and testing an inhalable preparation of the second-generation antipsychotic medication, Risperidone (RIS). Using an 8-stage Anderson Cascade Impactor (ACI), which is an FDA approved device for the pre-clinical evaluation of drug delivery by pulmonary administration. The following uses the ACI to perform an initial technical assessment pertaining to the feasibility of therapeutically-delivering a relevant dose of the atypical antipsychotic (Risperidone) for the treatment of schizophrenia. Two representative systems were used to assess the technical feasibility of therapeutically delivering Risperidone to the deep lung for systemic uptake: a commonly used and FDA approved jet nebulizer (PARI LC®) as well as an unapproved unregulated electronic cigarette (E-cig) as a delivery device, specifically the Joyetech eGO-C®.

Based on the previous literature explored to date, the approach of utilizing pre-existing drug administration behavior to address low adherence within the treatment population of interest (schizophrenia patients) has not been employed. Additionally, using the widely accessible electronic cigarette device as a platform for delivery and administration of an approved pharmaceutical class drug has not previously been used to pre-clinically investigate the technical feasibility of administering and delivering a therapeutically relevant drug and dosage by way of the pulmonary route.

First, in the Introduction (**Chapter 1**), I will introduce Schizophrenia and the experimental purpose, motivation and rationale. In **Chapter 2**, I describe the preliminary investigation into the technical feasibility of delivering Risperidone by inhalation for the treatment of schizophrenia. A jet nebulizer was investigated for validation, and an electronic cigarette was subsequently explored. A therapeutically relevant dosing regimen for deep lung delivered RIS was quantified by pharmacokinetic – pharmacodynamics model simulations. A solution of RIS was prepared, and ultraviolet spectroscopy (UV/Vis) was used to evaluate, describe, and quantify it (**Chapter 3**). The emitted RIS aerosol was characterized using an 8-stage Anderson Cascade Impactor to evaluate aerodynamic particle diameter distribution from a jet nebulizer (**Chapter 4**) and electronic cigarette (**Chapter 5**). The technical feasibility was experimentally assessed for drug stability via ultraviolet-visible (UV/Vis) spectrophotometry, and for delivered dose within the therapeutic window via aerosol characterization using an 8-stage Anderson Cascade Impactor (Chapter 6).

1. INTRODUCTION

1.1 SCHIZOPHRENIA

Schizophrenia is a complex and debilitating psychiatric disorder characterized by heterogeneity of symptoms, disease course and outcome. It is associated with an elevated mortality rate that is estimated at two to three times higher than the general population, with premature deaths attributed to both natural and unnatural (suicide, homicide, accidents) causes (7-9). Rates of disability and somatic comorbidity are increased, and patients with schizophrenia are at more than a twofold greater risk of diagnosis with diabetes, COPD, influenza and pneumonia (10). Impairments in executive functioning are a primary source of disability, and these appear to start early in the course of illness and remain stable, irrespective of symptomatic improvement (4, 11). The disease trajectory does vary, but for many patients tends to be chronic and refractory, with relapse following complete recovery reported in 65-90% of patients (4, 12-15). Residual symptoms after remission are common, and chronic deterioration across the life course is a trend reported in a subset of roughly 30-43% of cases (16, 17).

1.1.1 Symptomology

Schizophrenia is characterized by positive, negative, and cognitive symptoms, and is defined diagnostically by the occurrence of psychosis. Symptoms must be accompanied by social or occupational dysfunction with continuous signs of disturbance for 6 months or more to meet the diagnostic

criteria published in the Diagnostic and Statistical Manual of Mental Disorders (DSM-IV-TR, DSM-V; American Psychiatric Association, 2000, 2013). Positive symptoms are those that are typically associated with psychosis, including delusions, hallucinations, reality distortions and paranoia. Negative symptoms refer to the absence or diminishment of affective and cognitive functions, or to deficits in normal functioning. Examples of negative symptoms include social withdrawal; loss of interest, motivation/initiative (avolition), or ability to experience pleasure (anhedonia); blunted affect; and difficulty with abstract thinking. Cognitive symptoms of schizophrenia include deficits in working memory, attention, motor skills and executive functioning. The severity of different symptom clusters varies both across patients and throughout the course of the illness.

1.1.2 Antipsychotic Drugs

The dopamine hypothesis of schizophrenia proposes that an excess of dopamine in the limbic system is responsible for positive symptoms, while dopamine function in the mesocortical pathway may be responsible for negative symptoms. Pharmacotherapy targeting the dopamine system is widely accepted as the standard of care in the treatment of schizophrenia. Antipsychotic medications are the first-line treatment essential in limiting psychotic symptoms and reducing the risk of relapse (18-20).

Antipsychotics are divided into two catagories: first generation, also called typical antipsychotics and second generation (SAGs), also called atypical

antipsychotics (AATs). AATs differ as they work by targeting the dopamine D_2 receptors as well as the receptors for serotonin and norepinephrine, while first-generation antipsychotics work by blocking the D_2 receptors only (21, 22). Additionally, atypical antipsychotics (second generation) cause fewer side effects than their first-generation "conventional" predecessors, particularly with respect to serious life-altering extrapyramidal symptoms [EPS]. However, both generations are associated with long-term health risks including obesity and cardiovascular disease, and are often accompanied by limiting side-effects: extrapyramidal symptoms, weight gain, sexual dysfunction, anhedonia and sedation (23).

Antipsychotics are typically administered once or twice daily, as an orally ingested tablet for subsequent absorption and delivery from the gastrointestinal tract. Recent developments have also introduced long-acting injectable antipsychotic formulations (LAIs), which are administered every two to four weeks (23-26). LAIs were proposed with the intent to address low treatment adherence within the patient population (27). Less than 10% of individuals who commence LAIs in an inpatient setting continue using LAIs within 6 month as an outpatient (24), leaving treatment adherence as one of the most serious challenges in the treatment of schizophrenia.

Risperidone (Risperdal®, RIS) is a well-studied AAT, which is thought to selectively antagonize the dopamine receptors in the limbic system, treating positive symptoms, and produce a selective serotonin blockade in the mesocortical tract, treating negative symptoms (28, 29). Risperidone is indicated

for the treatment of schizophrenia in adults with a recommended (oral tablet, standard of care) target dose of 4-mg to 8-mg per day (efficacy demonstrated for the orally ingested tablet doses of 4-mg – 16-mg), taken once or twice daily (30).

1.2. EXPERIMENTAL PURPOSE MOTIVATION AND RATIONALE

One of the most serious challenges in the treatment of schizophrenia is poor adherence to psychopharmacological treatment. Schizophrenia is associated with the lowest rate of treatment adherence among psychiatric disorders. Literature estimates of non-adherence range between 58-75% (31-35). Poor adherence to treatment in patients with schizophrenia is associated with increased relapse rates, more frequent hospitalizations, higher levels of treatment-refractory residual symptoms and poorer long-term functioning and overall outcomes (36, 37). Alternately medication adherence is positively associated with patients' well-being (38). The causes of poor adherence in schizophrenia are varied and include medication side effects, stigma, poor insight into illness, uncertainty about the benefits of treatment and impaired memory (23). In general, medication adherence increases with patients' acceptance of and positive attitude towards the treatment (36).

The rates of smoking in patients with chronic schizophrenia range from 70 to 90 percent compared to 20 percent of the general American population (39-41). Considering its high prevalence, inhaled drug administration may be associated with increased acceptability in this population over standard tablet

ingestion, reducing the connection of treatment to social stigma, illness, and distrust of treatment.

Given the nature of drug (nicotine) dependence, smoking is a highly-ingrained behavior. Replicating this method of administration for the delivery of antipsychotics may increase adherence rates by leveraging the chosen drug administering behavior (smoking) to incorporate a therapeutically beneficial one. Cognitive deficits in memory and general executive functioning are associated with schizophrenia (4, 42, 43), thus the acquisition of new behaviors and/or habitual routines are hindered, as is adherence to treatment regimens. Administering treatment by inhalation circumvents the barrier of behavioral acquisition as it parallels an existing behavior that is reliably ingrained and routinely performed with frequency.

A breath-actuated delivery system of thermally generated aerosols has been investigated using Loxapine, a typical antipsychotic, for the treatment of in-patient acute agitation (44-46). ***Inhalation has not been employed previously as an alternate for the routine administration of antipsychotic medications in the treatment of psychiatric illnesses, such as schizophrenia.***

1.3 PULMONARY DELIVERY

1.3.1. Advantages of Pulmonary Delivery Route

Inhaled (pulmonary) administration offers several advantages over the pre-existing administration methods: the orally ingested tablet (1 - 2 tablets/day) (47),

which is the current standard of care, and the increasingly available Long-Acting depot Injectable or LAIs (1 injection/2-4 weeks) (19).

Inhalation is a noninvasive needle-free system (48) that is associated with relative ease and comfort (49), and has the convenience of self-administration compared to the required clinical administration of LAIs. Unlike intravenous bolus injections and inhalation, LAIs' have a slow drug-release mechanism requiring an initial period, during which oral treatments are continued until therapeutic exposure levels are attained. By comparison, the pulmonary route's unique strength is its rapid systemic drug absorption profile, and ensuing therapeutic effect, that closely parallels intravenous bolus injections (50).

As the standard of care, oral tablet ingestion is associated with poor absorption and high metabolism. Comparatively, the lungs' low enzymatic environment combined with its extensive, highly permeable, absorptive surface area allows for rapid systemic uptake of drug. Because the pulmonary route of administration bypasses the liver, drug bioavailability and drug losses associated with hepatic first-pass metabolism is avoided. Furthermore, systemic drug delivery by pulmonary administration is not impacted by dietary complications, or interpatient metabolic differences; as a result, its absorption kinetics are reproducible (50, 51).

1.3.2 The Pulmonary Route for Systemic Drug Delivery: Lung Physiology, Aerodynamic Particle Diameter Size, And Systemically Available Delivered Dose

The lung's airways have a hierarchical structure that stem from the trachea, which divides to form the left and right bronchus. The bronchi supply oxygen to the left and right lungs, where they divide and further subdivide into increasingly narrow airways called bronchioles. Terminal bronchioles end in alveolar ducts and alveolar sacs. The alveolar surface supports gas-exchange, promoting the free transfer of oxygen and carbon dioxide across the lung's epithelial walls to and from the bloodstream by the process of diffusion. The lung's several million alveoli, dedicated to this gas-exchange process, account for 95% (approx. 81 m^2) of the lung's surface area, with thin epithelial walls ranging from 0.1-0.5 micrometers in thickness. The vast surface area and thin penetrable barriers to the bloodstream allow for the rapid systemic absorption profile of pulmonary administration (22, 51, 52).

Systemically available drug absorption occurs in the alveolar region of the lung, which is referred to as the deep lung region in pulmonary drug delivery. Due to the physiological characteristics of the lung, aerosolized drug particulate's aerodynamic diameter is a prominent indicator of the pulmonary region of drug deposition. The deep lung region targeting systemic drug delivery is associated with the aerodynamic particle diameter of less than 2 - 3 micrometers (50). Thus, the mass sum of aerosolized drug corresponding to this aerodynamic particle size range will define the delivered dose. The delivered dose of aerosolized Risperidone, utilizing the jet nebulizer and the electronic cigarette as representative systems, will be evaluated for its therapeutic relevance (plasma drug exposure and corresponding therapeutic effect, pharmacokinetics –

pharmacodynamics). This will be a significant factor in the technical evaluation of feasibly delivering Risperidone for schizophrenia treatment by the pulmonary route.

1.4 EXPERIMENTAL OVERVIEW

This study was designed to examine the technical feasibility of delivering a therapeutic dose of RIS through inhaled administration. Medications can be aerosolized or converted into a mist for inhaled drug delivery using several different systems and mechanisms. Pharmaceutical aerosol devices can be broadly categorized by method of aerosol production: nebulizers, metered-dose inhalers (MDI), and dry power inhalers (DPI). These general categories can be further sub classified. For example, nebulizers are organized according to whether jet, mesh, or ultrasonic vibrations are employed for aerosol generation of liquid drug formulations. For the purposes of this study two aerosol delivery devices were selected for evaluation: a jet nebulizer and an electronic cigarette.

1.4.1 Representative System #1: The Jet Nebulizer

A jet nebulizer is the most common, conventional, and accessible pulmonary delivery device. It is frequently used for generating aerosol in preliminary drug studies. The jet nebulizer is the only FDA approved pharmaceutical aerosol delivery device that is approved for a variety of drug formulations. A jet nebulizer works by passing externally supplied compressed air into the nebulizer via a narrow orifice surrounded by the contained liquid drug

formulation. Aerosol production occurs as described by the Bernoulli principle (66). Conventional nebulizer systems use compressed air to deliver the aerosol continuously by using an apparatus or machine to increase air pressure whereby the liquid is vaporized upon release due to a rapid change in air pressure.

1.4.2 Representative system #2: The Electronic Cigarette

The electronic cigarette (e-cig) was first patented in 2004 as a cigarette alternative nicotine delivery device that is smoke-free and tobacco-free (53) . The e-cigarette has rapidly gained popularity with sales doubling from 2011 to 2012 to $500 million (54, 55). Top U.S. tobacco companies have purchased electronic cigarette brands. Despite their market popularity, E-cigs are unregulated by the FDA, there is little available research on their health impact, and they are known for inconsistent product quality. The e-cig delivers nicotine by inserting energy into a liquid to create vapor. It also simulates the behavior of smoking, which is socially acceptable to individuals who have smoke traditional tobacco products (56).

1.5 CHAPTER OVERVIEW

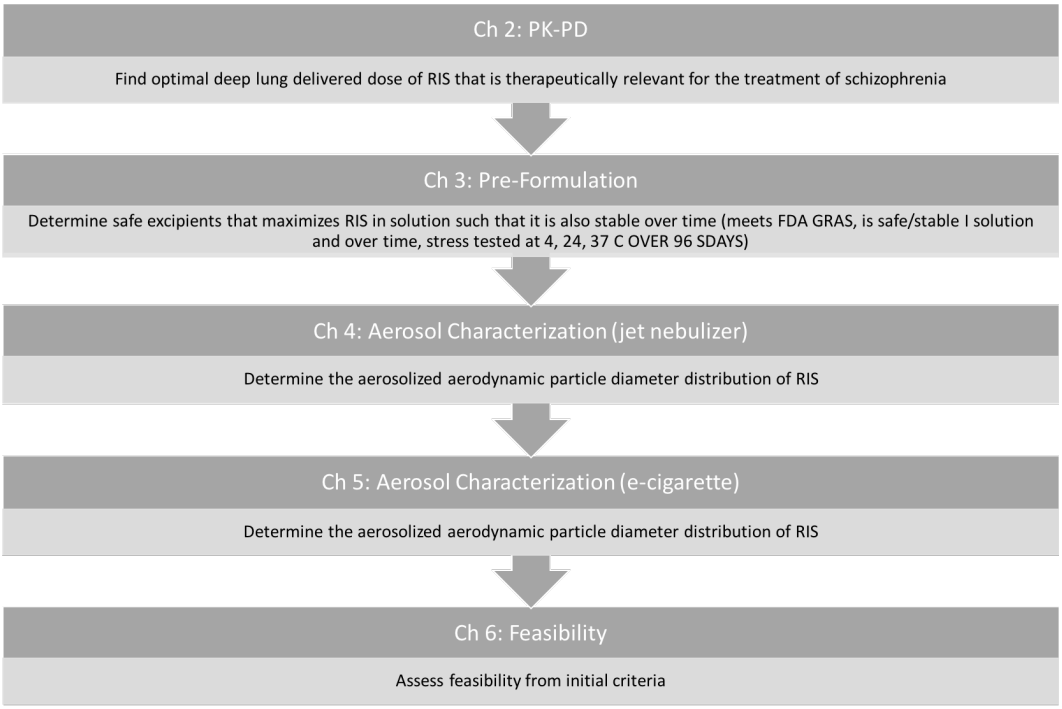

Figure 3 Chapter Objectives and Outline Flow Chart

In the above **Chapter 1**, the target treatment population (individuals with schizophrenia) was described along with the current pharmaceutical mediations and therapeutic treatments offered. The populations' low treatment adherence was mentioned along with the rationale and motivation of exploring the pulmonary delivery route for potentially addressing this issue. Following this Chapter objectives are described as follows (see Figure 5). The objectives of Chapter 2, 3, 4, and 5 as it pertains to the determination of technical feasible is outlined in Figure 6.

An optimal treatment-relevant dosing regimen (dose or drug mass and frequency) of Risperidone for the systemic delivery of Risperidone to the deep lung (< 3 micrometers) for the therapeutic treatment of schizophrenia was determined in **(Chapter 2) (50).** This was performed using a compartmental-model approach and computational simulations to evaluate the pharmacokinetics-pharmacodynamics of Risperidone.

A (pre)formulation assessment of Risperidone in (liquid) solution was described and assessed for feasibility - safety and concentration **(Chapter 3)**. The Risperidone solution was prepared using only FDA approved safe materials.

The Risperidone solution was aerosolized using a jet nebulizer (PARI LC®) (Chapter 4) and an electronic cigarette (Joyetech eGO-C®) **(Chapter 5)**. An 8-stage Anderson Cascade Impactor, a well-recognized FDA approved preclinical device, was used to characterize the emitted aerosol based on the aerodynamic particle diameter distribution **(Chapter 4, 5)**.

In **Chapter 6**, technical feasibility of therapeutically delivering Risperidone by inhaled administration was assessed and discussed based on the criteria described and outlined in Figure 6 and described further in Figure 1 Chapter Objectives and Outline Flow Chart.

To assess technical feasibility (**Chapter 6**) the delivered dose of aerosolized Risperidone (< 3 micrometers) was compared to that of the optimal therapeutic dosing regimen in **Chapter 2**. Time of administration to deliver the

FEASIBILITY	
CRITERIA	**DESCRIPTION**
SAFETY	Drug remains stable in solution
	Drug prepared in solution use excipients that are FDA approved as safe for the given application
	Realistic storage conditions for drug stability
	Drug is stable after being aerosolized
EXPERIMENTAL DEVELOPMENT	Mass balance is within +/-15% of initial dose experimentation
	The solution – aerosol delivery device combination is functional with selected representative devices (jet nebulizer and electronic cigarette)
	ACI methodology is developed such that results are reproducible (mass balance is maintained)
AEROSOL CHARACTERISTICS ARE APPROPRIATE FOR THE DESIRED DELIVERED DOSE OUTCOME WHILE BEING PRACTICAL	The concentration of drug in solution is maximized to theoretically achieved the optimal delivered dose
	The delivered dose is achieved without surpassing the device's volume limitations
	The delivered dose is achieved within an administration time frame that is reasonable (<20 minutes, determined based on other nebulized administered drug time frames).

Table 2 Feasibility Assessment table criteria

required therapeutic dose to the deep lung was calculated and considered for feasibility. The safety of Risperidone before (**Chapter 3)** and after being aerosolized (**Chapter 4,5**) was assessed using UV/Vis to determine the presence of any drug degradation products. Technical feasibility was additionally determined based on the stability (as an initial measure of safety) and concentration of the prepared Risperidone solution (**Chapter3**).

This study will assess the technical feasibility of systemically delivering a therapeutically relevant dose of risperidone for the treatment of schizophrenia by inhaled administration.

To the best of my knowledge, an atypical antipsychotic has not been evaluated for therapeutic outpatient treatment purposes. In addition, an electronic cigarette as a platform to delivered pharmaceutical agents for therapeutically-relevant treatment purposes has not been investigated (not including nicotine, and marijuana based substrates).

2. FINDING THE OPTIMAL DOSING REGIMEN (PK-PD)

The experimental exploration contained within this document is a proposal for delivering an existing drug via a delivery route that has yet to be explored or offered with respect to this drug and its related treatment population of schizophrenia, which is of focus here within. Thus, a therapeutically relevant dosing regimen for the population of interest, those with schizophrenia, relating to the delivery route of interest – the pulmonary route given inhaled administration - must be determined. The following chapter looks to determine the optimal deep

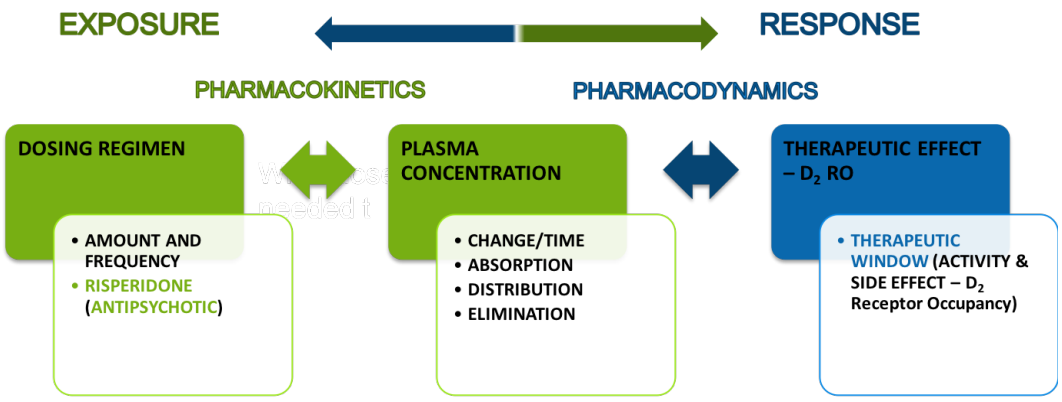

Figure 7 Pharmacokinetic--Pharmacodynamic (PK-PD) Relationship

lung delivered dosing regimen (available for systemic uptake and delivery) for the given drug and treatment population of interest (Risperidone and Schizophrenia). A preliminary exploration was pursued. Within the field of drug discovery this typically relates to an initial exploration and modelling of drug exposure and its

related effect. This can be studied by Pharmacokinetics (PK) and pharmacodynamics (PD) shown in Figure 7 Pharmacokinetic--Pharmacodynamic (PK-PD) Relationship.

Pharmacokinetics (PK) describes the movement of drug through the body and pharmacodynamics (PD) describes the branch of pharmacology, which is concerned with the effects of drugs (therapeutic and toxic thresholds) and the mechanism of their action. The PK model for our RIS delivery has to take the uptake system for inhaled drugs, namely the lungs into account. In addition, the PD model must describe the concentration from the lungs to the therapeutic effect and is therefore based on receptor binding in the brain. In this chapter I introduce the PK-PD model, which I developed to study the therapeutic effect of RIS through inhalation. I adjusted and validated this system through previously published data on RIS.

2.1 INTRODUCTION

RIS is described as a selective monoaminergic antagonist with a high affinity for the dopamine D2 and serotonin 5-HT2A receptors (57-59). RIS metabolism takes place primarily in the liver by cytochrome P450-2D6 (CYP2D6) via alicyclic hydroxylation and oxidation N-dealkylation (60). This results in the production of another recognized antipsychotic agent, 9-hydroxyrisperidone or Paliperidone (PALI). The sum of RIS and PALI plasma concentrations is called "active moiety" and is clinically relevant. This means both components are critically responsible for the therapeutic effect shown to be effective in treatment of positive, negative and affective symptoms of schizophrenia (61, 62).

In general, the plasma concentration-time profiles of RIS and PALI differ. PALI has a longer half-life than RIS. The systemic absorption of an IV bolus of RIS is instantaneous and so the deep-lung-dosed RIS is assumed to be instantaneous as well (63, 64). In contrast PALI's absorption is slower as it depends on its rate of production from metabolized RIS. RIS and PALI are predominantly excreted by non-renal and renal clearance respectively, which results in a higher clearance rate for RIS (62). The PK compartmental model must therefore account for both RIS and PALI separately as the rate of drug clearance needs to be accounted for and determined for separately.

Humans are phenotyped as poor, intermediate or extensive metabolizers. CYP2D6 enzymatic activity and corresponding PALI production varies significantly between individuals due to genetic polymorphism, whereas active

moiety remains relatively consistent across all those metabolic phenotypes. Extensive metabolizers produce greater amounts of PALI from RIS and make up 80% (the majority) of the population. Therefore, I will concentrate on the data of extensive metabolizers in this thesis (21, 65).

For the PD model it is important to know that the PD properties of RIS and PALI are similar with regard to potency (equipotent), activity, and the ratio of antagonistic interaction with the 5-HT2A and D2 receptors (51,55). D_2 receptor blockade, associated with antipsychotic medications, has been hypothesized as the mechanism of therapeutic action as it relates to the treatment of schizophrenia and psychotic symptoms. Therefore, previous literature measures therapeutic effect of antipsychotic medications by D_2 receptor occupancy (D_2RO %) resulting from measured plasma drug concentration (59, 66).

In this thesis, we use a therapeutic window based on the quantifiable measure of D_2RO% occupancy, to define the upper and lower drug exposure related therapeutic effect thresholds. The defined therapeutic window is then used to qualitatively assess and determine an optimal dosing regimen (parameters of dose amount and frequency) to maximize therapeutic effect while minimizing risk associated with drug exposure. Previous literature of antipsychotic medications effect has defined the therapeutic window for the treatment of schizophrenia as having upper and lower thresholds of 60% and 80% D_2RO% occupancy respectively (60-63). The lower limit defines the minimum drug concentration required to achieve clinically therapeutic effect. Previous literature typically

associates 60% D_2RO for the lower window threshold. The minimum threshold of 60% occupancy is believed to represent a pharmacologic level for the majority of responders, however therapeutic response has been observed at lower occupancy values (67, 68). The lowest limit of D_2RO while remaining therapeutically effective appears less concrete with more recent evidence suggesting that clinical effect can be achieved with significantly less than 60% occupancy. Phase 3 clinical trials initially suggested orally administered RIS dose of 6-mg/day (69, 70).

The upper drug exposure-effect limit is defined as 80% occupancy, based on the significant increase in life-impacting drug side-effects associated with antipsychotic mediations, when drug plasma concentrations levels are above this limit. Values exceeding 80% are associated with increased occurrences of Extra Pyramidal Symptoms (EPS) (60-63). EPS are defined as often-irreversible movement related disorders that range from chronic involuntary muscle movements (tardive dyskinesia) to brain damage. However, this limit is flexible as indicated by the nature of data collected primarily from inpatient units showing results of only the most seriously impacted patients.

$$D_2\ \text{Receptor Occupancy}\ (\%) = \frac{(\ \text{Occupancy}_{\text{Max.}}\ )^{*}\ [\ \text{Concentration}_{\text{ActiveMoiety}}\ ]}{(\ K_d + [\ \text{Concentration}_{\text{ActiveMoiety}}\ ]\ )}$$

Equation 1 PD therapeutic effect equation used to determine D2 RO% based on plasma concentration of the active moiety simulated over time from the compartmental model

In summary, in this thesis I define the therapeutic window of 60% - 80% D_2RO to observe the relationship between simulated results of iteratively varied dosing regimen parameters (dosing amount and frequency) pertaining to drug exposure (plasma concentration over time) and resulting drug effects (D_2RO % occupancy vs drug plasma concentration) using Equation 1. The upper and lower thresholds serve as a means of evaluating and determining optimal dosing regimen parameters coinciding with optimal dose amount and dosing frequency. The optimal dosing regimen was determined and concluded based on optimizing the drug plasma exposure – therapeutic effect within the bounds of the therapeutic window as graphically and qualitatively observed (67, 68).

2.2 METHODS

The described PK-PD model was validated by simulations, which reflect the biological and physiological processes of extensive metabolizers (model population, see above (62). The model was simulated for a comprehensive array of dosing parameters. The parameters that maximized pharmacological effect, while minimizing potential toxicity, were selected for the optimal dosing regimen of aerosolized RIS.

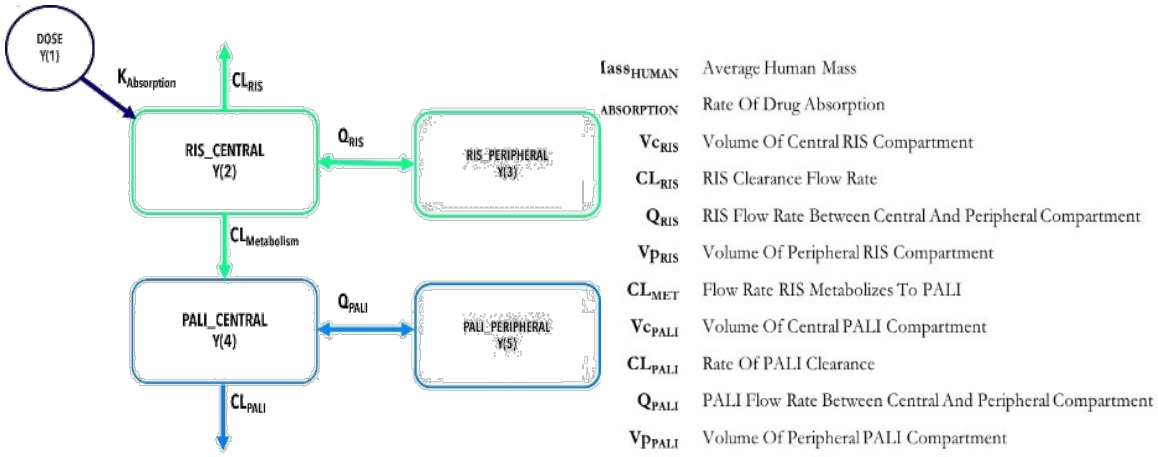

Figure 8 Depiction of the four compartment PK model of RIS. Labeled coefficients are shown and their definitions explained on the right. Model indicatesvolumetric flow between compartments and clearance out fo the body. The Dose (EGO(1)) is labeled and once model has been validated will be the chapter objective to determine the dose of RIS to be delivered to the pulmoanry regions of the lung associated with systemic uptake while maximizing therapeutic exposure based on PK drug exposure and associted PD therapeutic effect; defined as the optimized dosing regien

2.2.1 PK Model Validation

A PK model of RIS was described, validated and simulated to determine the optimal dosing regimen for deep-lung-delivered RIS. The PK model was based on previous literature of RIS PK analyses, PK principles, and the theory of mass transfer. In addition, I applied the compartmental approach to the PK analysis (63, 64).

The PK model of RIS was described by a four-compartment model which accounted for PALI's distinct PK profile (Figure 8) from RIS.. Each compartment's drug concentration was expressed as a function of time and their

$$dY(1) = -\text{Dose}_{RIS}$$

$$dY(2) = -(CL_{RIS}/Vc_{RIS})*Y(2) - (CL_{MET}/Vc_{RIS})*Y(2) - (Q_{RIS}/Vc_{RIS})*Y(2) + (Q_{RIS}/Vp_{RIS})*Y(3)$$

$$dY(3) = +(Q_{RIS}/Vc_{RIS})*Y(2) - (Q_{RIS}/Vp_{RIS})*Y(3)$$

$$dY(4) = +(CL_{MET}*Y(2))/(Vc_{RIS}) - (CL_{PALI}/Vc_{PALI})*Y(4) - (Q_{PALI}/Vc_{PALI})*Y(4) + (Q_{PALI}/Vp_{PALI})*Y(5)$$

$$dY(5) = +(Q_{PALI}/Vc_{PALI})*Y(4) - (Q_{PALI}/Vp_{PALI})*Y(5)$$

Equation 2 Equations defining the change of mass flow of drug (RIS or PALI) over time. Equations were used to describe compartment model and coefficients were solved for numerically by comparing ouptut of the central RIS, PALI, and active moiety concentrations over time against clinically obtained plasma data. The model was validated when coefficiencts and graphcial output werecomparably similar with reasonble likeness for the purpose of this paper.

differentiated equations (see equations) were computationally solved using Gear's Method (71). The resulting concentration-time functions were simulated using Matlab to numerically solve the equations and produce the corresponding concentration-time output of RIS, PALI, and the active moiety.

The model was initially simulated using pre-clinical PK coefficients previously defined in rats by Kozielska et al (59) defined in Equation 2. Afterwards coefficients for human mass and the human central RIS and PALI compartment volumes were defined according to literature-established clinical values (59, 60). Concentration-time profiles of RIS, PALI, and the active moiety for extensive metabolizers' were extracted from the clinical data reportd in the study by Huang et al (60, 62). These clinically obtained concentration-profiles were measured from plasma samples collected over 72-hours, after the intravenous adminstration of a 1-mg RIS dose. In the current study, simulated

concentration-time profiles for RIS, PALI, and the active moiety were plotted

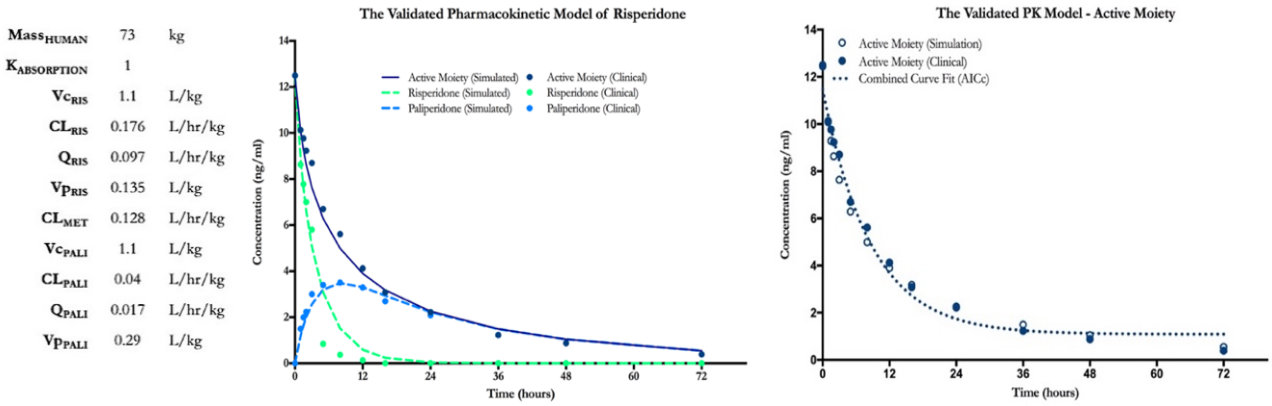

Figure 9 Validated model results graphically showing final coefficient values. The active moiety will be for determining PD output and optimized dosing regimen. Thus the model approximating active moiety output was placed above the independent RIS and PALI conc. outputs

over 72-hours against corresponding clinical data (60).

In an iterative process, PK model coefficients were adjusted and simulated, then graphically compared to the respective concentration-time clinical profiles, and subsequently re-adjusted to optimize the comparative output proximity. The iterative process was continued until the proximity of the simulated concentration-time profiles to the corresponding clinical profiles for RIS, PALI, and the active moiety were maximized (Figure 9). The model was validated when simulations reflected clinical concentration-time data, and therefore approximated physiological absorption, metabolism, and clearance of RIS (Figure 9).

2.2.2 PD Model & Validation

Under the assumption that a linear relationship between RIS plasma and brain concentrations exists, the simulated active moiety concentrations from the validated model were used to determine D_2 receptor occupancy by the law of mass action, in Figure 9. The maximum receptor occupancy was assumed to be 100%. The dissociation constant (K_d) is defined as the concentration at which 50% of receptors are occupied by the drug. Nyberg et al experimentally determined the K_d for RIS as 6.87 ng/ml based on clinical PET scans measuring D_2 receptor occupancy with respect to the concentration of RIS using Equation 1 (69).

Based on the described equation (Equation 2), simulated active moiety concentrations were used to calculate D_2RO over time, and results were graphed (Figure 10). Two dosing parameters were included in the model and defined as: the dosing amount of systemically delivered RIS, and its administered or delivered frequency. The optimal dosing regimen was determined based on maintained exposure within the therapeutic window (60%-80% D_2RO) at steady state, corresponding to 10 ng/ml and 27 ng/ml as defined by Nyberg et al. (69). The exposure-response profiles were also characterized with respect to time: until minimum therapeutic threshold was breached, outside of therapeutic exposure if considerable, and until steady-state was achieved.

2.3 RESULTS & DISCUSSION

Based on the validated PK-PD model simulations, the dosing regimen that

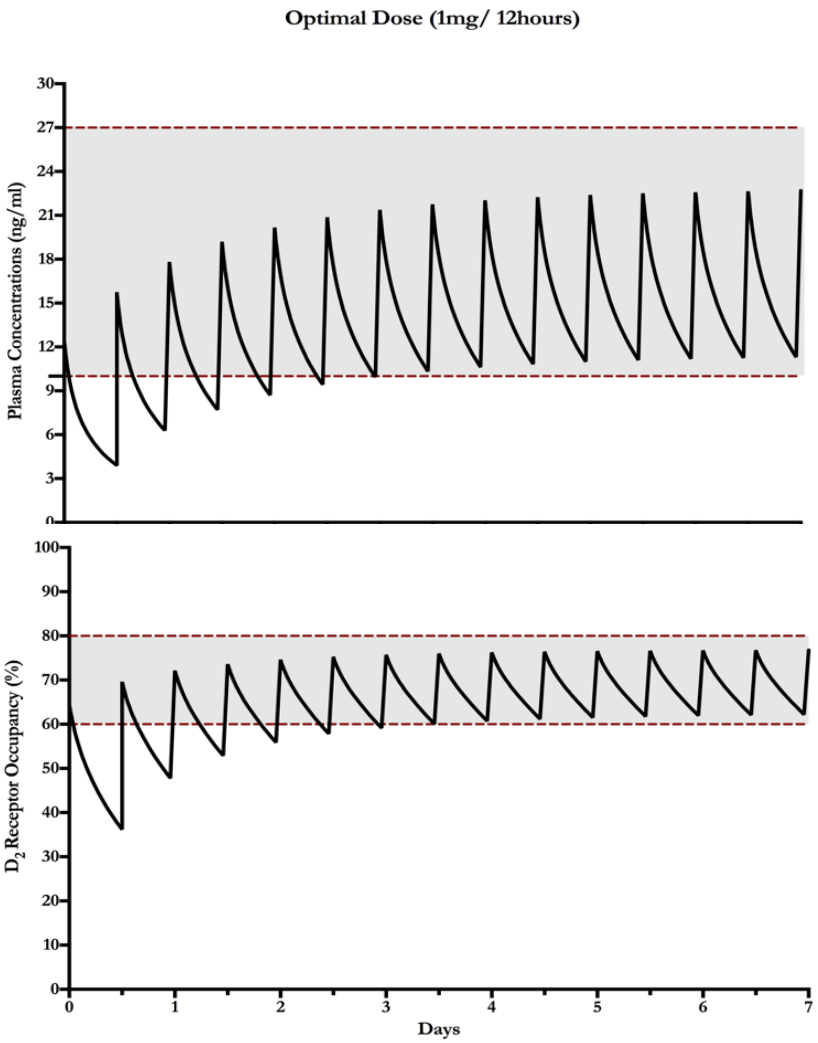

Figure 10 OPTIMAL DOSING **REGIMEN OF 1MG/12HRS simulated output of exposure vs time and D2RO effect over time. Both plots shown with a dotted red line the respective therapeutic window minimum and maximum associated**

maximized therapeutic effect based on RIS plasma-concentration or exposure window was found to be:

1 MG/12-HOURS RIS DELIVERED TO THE DEEP LUNGS

Steady state exposure within the therapeutic window (62-77% D_2RO) was

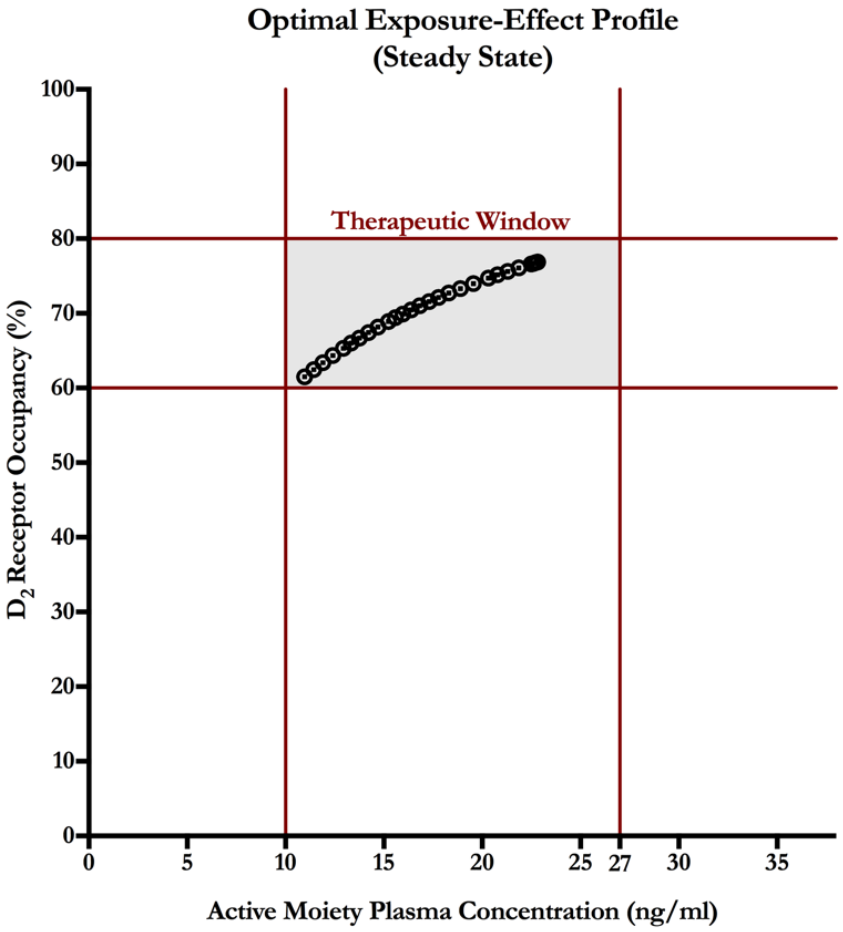

Figure 11 The exposure-effect profile of the optimal dosing regimen - 1 mg/12 hours - graph at steady state and shown together with the therapeutic window for reference

achieved after the 5th day, or after 10 doses administered as **1 mg/12 hours**.

Dosing parameters were iteratively adjusted both in dosing amount and frequency. The optimal dosing regimen of 1-mg/12-hour was determined after assessing extensive methodological dosing parameter permutations and respective

simulations. Dosing parameters (dose amount and frequency) were simulated using the defined, validated 4-compartment PK-PD model. The optimal dosing regimen selected was 1 mg dosed every 12-hours or twice daily. The optimized dosing regimen was determined based on the exposure-effect profile, which was qualitatively observed to remain within the defined therapeutic window thresholds defined as between 60% to 80% D_2RO.

` Therapeutic exposure was maintained on day 1 for a total of 3 hours; on day 2 for 13 hours and on day 3 for 20-hours respectively. After day 3 or the 6^{th} dose, therapeutic D_2RO effect levels remained above the minimum baseline threshold for all time points. After day 3, relatively small changes in exposure-effect profile were observed until steady state was ultimately reached after day 5 or the 11^{th} dose, after which the exposure-effect profile remained unchanged. At

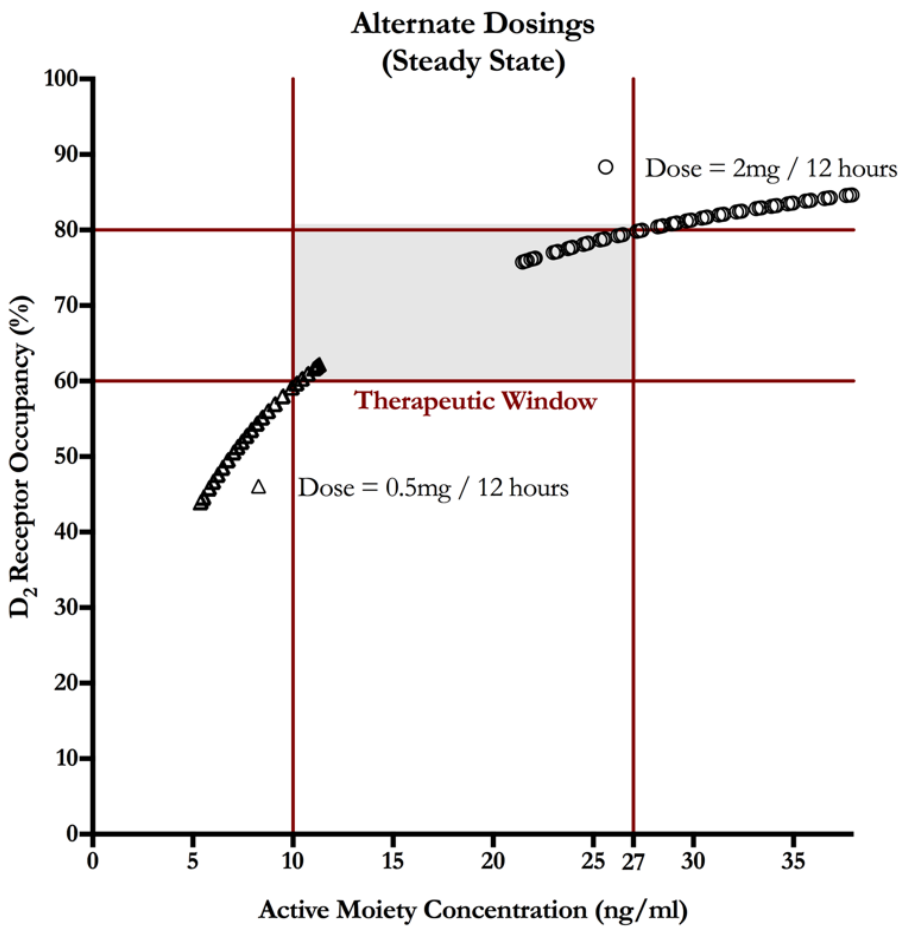

Figure 12 The exposure-effect profile of the alternate dosing regimens – 0.5 & 2 mg/12 hours - graphed at steady state and shown together with the therapeutic window for

steady state, therapeutic D_2RO effect oscillated between 62-77% with corresponding active moiety plasma concentrations of 11 to 23-ng/ml.

The dosing regimen of 1 mg every 12 hours was determined to be optimal because exposure was maintained within the defined therapeutic window of 60-80% D_2RO. The optimal dosing regimen was selected given the D_2RO of 62%-77% at steady state, which indicated drug exposure was above the minimum level associated with therapeutic effect while remaining below the D_2RO upper threshold above which the risk of serious side-effects is significantly increased.

Figure 12 shows examples of alternate dosing regimens regarding the amount administered. Dosing at 0.5 mg/12 hours resulted in steady state exposure levels below the minimum therapeutic threshold of 60% D_2RO (10 ng/ml plasma concentration). Dosing at 2 mg/12 hours resulted in steady state exposure levels exceeding the maximum therapeutic threshold of 80% D_2RO (27-ng/ml plasma concentration). These sample simulations, in addition to other simulations performed, support the determination of the optimal dosing regimen of 1-mg/12 hours.

Comparing model simulations of alternate dosing regimens indicates the model is highly sensitive to small changes in dosing parameters. This can be observed qualitatively in Figure 12, which displays a comparison of dosing amounts around the optimal dose of 1 mg (0.5-mg and 2-mg dosed at the same frequency of 12 hours). The graphical representation indicates notably different profiles both extending considerably outside the bounds of the defined therapeutic window despite the slight variations in dosing amount parameter values.

2.3.2 LIMITATIONS & FUTURE CONSIDERATIONS

The model was validated based on the proximity of the validated-model's simulated output ([RIS]-time, [PALI]-time, [AM]-time) with respect to the clinical data of extensive metabolizers (only) that was extrapolated from a study by Huang et al (60). This study has been extensively cited and referenced, however it has a small sample size and minimal patient diversity. Approximately 80% of the general population is an extensive metabolic phenotype (62).

Subsequently, subjects were predominantly extensive metabolizers. Intermediate and poor metabolizers were each represented by one subject, and a single corresponding data set (62).

A 4-comparmtent model was selected to represent to pharmacokinetic profile of Risperidone (plasma concentration(s) vs. time). The PK-PD of Risperidone has been researched previously within the literature. The determined validated model coefficients were not numerically representative of accurate values. They were representative of the simulations of the (change in) concentrations (RIS, PALI, AM) over time. While coefficient values may not be numerically accurate their simulated output is representative of the physiological pharmacokinetic processes of Risperidone as it moves throughout the body over time. Simulations were adjusted and evaluated based on a 4-comparmtent model of Risperidone.

The validated compartmental model coefficients were determined based on the proximity of model simulated output against clinically extrapolated data plasma concentration(s)-time data for subject with an extensive metabolic phenotype. Extensive metabolizers comprise most of the population.

In addition, the pulmonary route has a reproducible absorption uptake kinetics and is independent of metabolic differences, which is in contrast to oral administration and the gastrointestinal delivery route (50). The active moiety has a pharmacokinetic profile, plasma concentration – time, that remains consistent despite different metabolic phenotypes (62). Nonetheless, further investigation and assessment of the optimal dosing regimen pertaining to intermediate and poor

metabolizers should be evaluated given their vulnerability to exceeding the upper therapeutic window threshold associated with drug toxicity.

The PK model coefficients were validated using clinical data for extensive metabolizers. Intermediate and poor metabolic phenotypes were not considered. Extensive metabolizers comprise 80% of the general population (60). The validated model was considered acceptably representative of the human physiology for this study's object given the assumption that the literature clinical extensive metabolizer data was representative of the population.

The validated PK model does not suggest the selected coefficients are numerical accurate values. The PK model simulates the concertation-time profiles that approaches or approximates the physiological data as represented by graphical, clinically derived, data points. Pulmonary administration was modeled under the assumption that pulmonary deep lung drug delivery has an instantaneous rate of systemic absorption paralleling that of an IV bolus (which numerically translates to have a $Ka = 0\ hours^{-1}$ with a corresponding bioavailability of 100% for modelling and simulation purposes). There are additional factors beyond the scope of this research that contributes to pulmonary drug uptake in the deep lung region which have not been considered here within – an example would be the electric charge of drug particulates but the process of drug uptake is more complex than accounted for in most preliminary models including the one aforementioned (72, 73)

2.4 CONCLUSION

A 1-mg/12-hours dosing regimen of RIS delivered to the deep lung regions (for systemic availability) was concluded to be the optimal dosing amount and frequency. This dosing regimen ascertains exposure-effect profile within the therapeutic window such that D_2RO levels are above the minimum required to achieve therapeutic effect and below the D_2RO level associated with severe life altering side-effects as well toxicity and other impacts that risk safety. Future experiments may evaluate dosing regimens using data from all metabolic phenotypes as opposed to only those of extensive metabolizers.

Subsequent chapters will describe a RIS solution that was designed to be aerosolized in order to experimentally assess the feasibility of delivering the determined optimal deep lung dose of 1-mg.

3. PRE-FORMULATION EVALUATION

3.1 INTRODUCTION

A RIS solution for pulmonary drug delivery using the representative device (jet nebulizer and electronic cigarette) was designed to meet the following required criteria : solution is compatible with representative delivery device to functionally aerosolize and emit drug, optimal drug-solution concentration is achieved, the maximized solution concentration and emitted aerosol volumetric flow rate can theoretically meet the delivered dose criteria of 1-mg to the deep lung (< 3 micrometers), the drug remains stable pre- and post- aerosolization in order to determine the drug delivered as being safe and pharmacologically relevant (integrity) for therapeutic purposes.

Safety was defined by physical and/or chemical stability of the active pharmaceutical product against anticipated degradation processes.. Stability was determined based on the lack of newly formed chemical products suggested by new peak formations against the baseline collected from Ultraviolet-visible (UV/Vis) spectrophotometry readings. In summary, no peak new peak formation suggested stability based on the lack of degradation evidence.

Risperidone (RIS) is a benzisoxazole derivative with the chemical designation 3-(2-[4-(6-fluoro-1,2-benzisoxazol-3-yl)-l-piperidinyl]ethyl)-6m7m8m9-tetrahydro-2-methyl-4H-pyrido pyrimidin-4-one and molecular formula [C23H27FN4O2] (57, 58, 74). Risperidone is a Biopharmaceutics

Classification System (BCS) Class II compound, which by definition have high permeability and low solubility (75). Risperidone is soluble in 0.1 HCL and Methanol, insoluble in NaOH and Acetonitrile (76) and practically insoluble in water (sigma Aldrich) (77, 78).

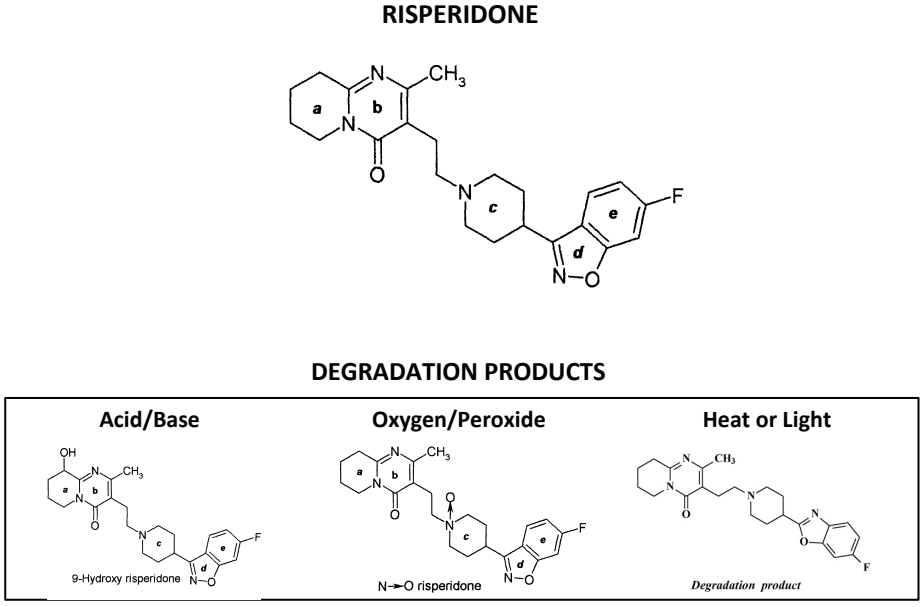

Figure 13 molecular structure of Risperidone. molecular structure of RIS known degradation products including 9-hydroxy risperidone or PALI. (1, 2)

Tomar et al (2004) characterized two degradation products of RIS after exposing it to acid, base, and peroxide for eight hours (1). RIS subjected to acid and base environments resulted in the structural presence of a hydroxy group in the degradation product, due to the formation of 9-hydroxy-risperidone

(Paliperidone or Pali, the active metabolite of RIS). RIS was demonstrated to be susceptible to peroxide degradation [oxidation], leading to the formation of N-Oxide in the piperidine ring (1, 79-81). Thermal or photolytic degradation of RIS in tablet powder form results in a pale yellow impurity, described by the rearrangement of RIS' isoxazole ring to the corresponding oxazole moiety (2). Refer to Figure 13. Limited information was found regarding the impact of these degradation processes on the pharmacological effect of RIS.

Several analytical techniques for RIS analysis have been described in the literature including Ultraviolet-visible (UV/Vis) spectrophotometry, which was the analytical method applied here using the Beer-Lambert Law for the quantitative determination of RIS (2, 76, 82). Ultraviolet-visible (UV/Vis) spectrophotometry measures absorption as function of wavelength.

Previous studies have validated UV/Vis for the identification and quantification of RIS and its degradation in pharmaceutical formulations (81). RIS is a UV-absorbing molecule with specific chromophores in its structure, and has characteristic absorption peaks at 240 and 280 nm (76). Using the Beer-Lambert Law, which describes the directly proportional and linear relationship between concentration and absorbance/optical density at a wavelength, calibration curves (absorbance vs concentration graphs) were constructed for determining the concentration of RIS in samples.

Several different techniques may be employed to solubilize a drug compound, including pH adjustment, cosolvents, complexation, microemulsions, self-emulsifying drug delivery systems, liposomes and emulsions. The use of

cosolvents was selected in the present study as the desired method for solubilization, and proper excipient selection was necessary for the optimization of RIS solubility. The combination of an aqueous solution with a water-soluble organic solvent is a common formulation for injectable drug compounds, and propylene glycol and ethanol were selected as solubilizing excipients (78).

The use of co-solvents selection was based on meeting requirements associated with safety and concentration maximization based on the previously determined optimal delivered dose to the deep lung of 1-mg found in Chapter 2.

Excipients, the inactive ingredients in drug formulations, were considered for use in the present experiment if approved by the Food and Drug Administration (FDA) ("Generally Recognized As Safe," GRAS) for use in inhaled solutions. Ethanol and propylene glycol are FDA GRAS approved excipients up to 25% vol/vol. In a study by Kumar and Pathak, a 3.5-mg/mL RIS solution was prepared using ethanol (95% vol/vol), propylene glycol and water (10:20:70 %vol/vol, respectively) (83, 84). In the present experiment, RIS was similarly prepared in a solution comprised of ethanol (95% v), propylene glycol, and water in a ratio of 25:25:50 %vol/vol/vol, respectively. The RIS solution was analyzed for degradation over time at various conditions (temperature, time) to assess drug stability.

3.2 MATERIALS & METHODS

3.2.1 MATERIALS

Risperidone (RIS) dry powder, Propylene Glycol, Purified Water, Ethanol (95%) were purchased from Sigma-Aldrich. Corning® 96 well plates, UV-transparent CLS3635 96 well plate, UV-transparent, acrylic copolymer, flat bottom, clear, non-sterile, 50/cs (Sigma). UV-VIS instrument.

3.2.2 METHODS

RIS solutions were prepared in concentrations ranging from 0.001-mg/ml to 7.500-mg/ml. 50-mg of RIS in fine white powdered form were received from Sigma Aldrich in a sealed amber colored glass vial. It was assumed that the mass of RIS reported by Sigma Aldrich was accurate. The selected solubilizing excipients, propylene glycol (PG) and ethanol (EtOH, 95% vol/vol), were combined in a plastic test tube in equal parts by volume (% vol/vol) and 5-ml was pipetted directly into the vial of RIS to make a 10mg/ml solution. This vial was then placed in an ultrasonic water bath at room temperature for 20-minutes to enhance the dissolution of RIS. Once solubilized, the 10 mg/ml RIS solution was transferred to a 10-ml plastic test tube and 5 ml of distilled water was added to make a 5 mg/ml solution (25:25:50 %v/v/v PG/EtOH/H2O). This 5-mg/ml solution was diluted for lower concentrations, and initial volumes of excipients were adjusted for concentrations higher than 5 mg/ml to maintain this formulation concentration.

UV/Vis generated data was used to analyze samples of solution at varying RIS concentrations and collect data for assessing stability. All samples were scanned in the range of 200-900 nm wavelengths at 5 nm increments, using UV-transparent 96-well plates holding 0.1-ml sample volumes. UV/Vis absorbance values of RIS solution samples were adjusted for the background solution excipients by subtracting the respective absorbance values of the formulation/solution base or vehicle from the readings containing RIS. The adjusted values were always used in calculation – to construct the absorbance-concentration calibration curves for analysis, the spectra profiles of freshly prepared RIS solutions at varying concentrations for stability assessment using UV/Vis profile comparisons, and generally all experimentally gathered sample data.

Calibration curves data were collected from solution samples whose concentrations ranged from 0.001-7.500-mg/ml as well as the formulation base (0 mg/ml RIS). Wavelengths of peak absorption were extracted from the literature and adapted for this application. Two calibration curves at wavelengths 280 nm (peak absorbance) and 315 nm were created to account for the range of solution concentrations. RIS concentrations of >1-mg/ml resulted in an oversaturated signal and background noise at the 280-nm peak wavelength, thus an absorbance-concentration calibration curve at 315-nm was required. This solubility curve was created such that concentrations >1 mg/ml could be quantified without needing to dilute the sample. In doing so the potential risk of re-solubilizing drug

particulates that are not in solution was omitted, and sample concentrations were more accurately quantified. Linear regression was used to confirm a linear concentration-absorbance relationship in accordance with the Beer-Lambert Law, and to define the calibration curve equation (85). Optical absorbance against concentration (calibration curves) were plotted at wavelengths of 280-nm and 315-nm.

The previously-defined calibration curve equations were used to calculate the concentration of samples of unknown RIS concentration based on their adjusted UV/VIS absorbance values at 280-nm and 315-nm. The equated concentration of RIS was used to determine the total mass of RIS in each sample of known volume.

A RIS solution of 5 mg/ml concentration was selected for subsequent experiments to determine the feasibility of a systemically delivered dose of 1 mg (see Chapter 2). This concentration was selected by considering information found in previous literature on: RIS' low BSC II solubility, drug loss as dead volume within the jet nebulizer delivery device, and drug loss associated with pulmonary delivery.

Fresh, independently prepared 5-mg/ml RIS solutions were sampled and adjusted absorbance values at 315-nm were computed using UV/Vis. Sample UV absorbance values were graphically plotted (red markers) on the calibration curve

at 315-nm. The additionally prepared 5-mg/ml RIS solution samples were qualitatively evaluated against the 315-nm calibration curve defined regression line for assessing its proximity to the defined regression curve. Multiple batch preparations of 5 mg/ml RIS solutions were prepared and sampled, absorbance measures were collected and points were plotted on the regression curve at 315-nm. A 5-mg/ml RIS solution was considered viable in the defined preparation as well as feasible for further experimental testing and use if sample points fell reasonably near the line regression equation defining the 315-nm calibration curve. Following this, temperature-time stress stability tests were performed on the prepared 5mg/ml RIS solution for further assessment and evaluation as it relates to its preparation.

Stability over time was assessed by performing temperature-time stress tests on the 5 mg/ml RIS solution in the mentioned preparation. Nine 0.8 ml volume samples a 5.3 mg/ml RIS solution (25%PG: 25% EtOH : 50%H2O vol/vol/vol) and three 0.8-ml samples of a 0-mg/ml RIS formulation base solution were collected and placed into 1.5-ml plastic test tubes using a pipette and sealed with parafilm wax. UV/Vis scans were taken of both the 5.3 mg/ml RIS solution and the 0 mg/ml RIS formulation base solution on day-0 to function as controls. One sample of fresh formulation base and three samples of 5 mg/ml RIS solutions were stored at temperatures of 4˚C, 24˚C, and 37˚C (4 separate test sample vials per temperature condition) on the 0^{th}-day of assessment. UV/Vis scans (200-900 nm, 5 nm increments) were taken for sample of all vials on the 7^{th}, 14^{th}, 31^{st}, and

96^{th} days being at stored condition (see Table 4). Stability was defined as the consistency of sample measures in both spectral profile shape and RIS concentrations relative to the control (at day-0). Calculations of concentration for measure and comparison were determined from samples absorbance measures at 315-nm.

3.3 RESULT & DISCUSSION

3.3.1 absorbance-concentration calibration curves (280nm and 315-nm)

Figure 14, shows spectra profiles over all concentrations of RIS solution between 0.004-mg/ml and 7.500-mg/ml. Profile are consistent with respect to shape across all sample concentrations and profile shapes vary in amplitude proportionally with differing concentrations of RIS solution samples. RIS spectra

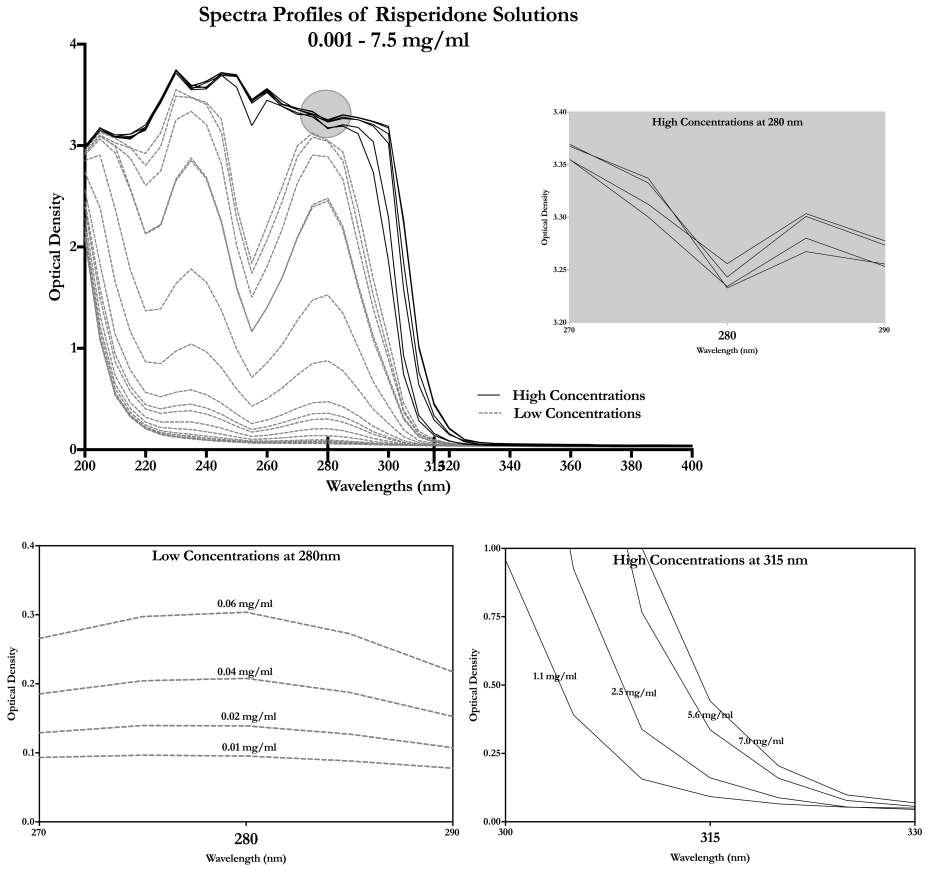

Figure 14 from left to right clockwise, spectra of RIS solution at varied conc., up-close depiction of oversaturated signal at 280nm at high conc., 280 nm and 315 nm showing proportional relationships between RIS concentration and absorbance

profiles were observed to have peak absorbance at wavelengths of 240-nm and 280-nm. These peak absorbance wavelengths were described as identifying characteristic markers of RIS in the previous literature. Based on the previous literature the RIS solution being evaluated and method of evaluation was accurate in its ability to identify and characterize the molecule of RIS (76, 82).

The absorbance-concentration curve at 280-nm was plotted for

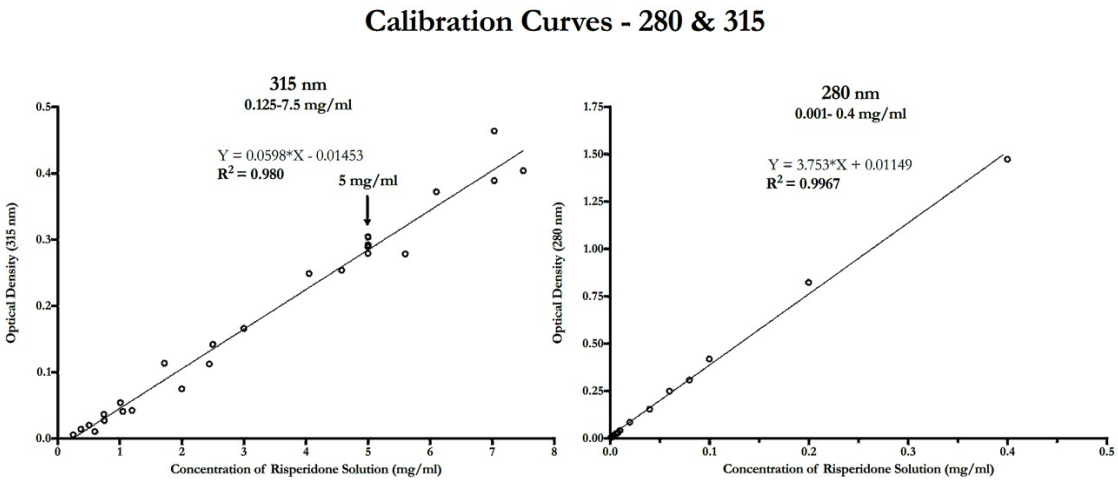

Figure 15 Absorbance-concentration curves for different concentration ranges of RIS in solution at 280 nm and 315 nm. Linearity was observed and regression line curve equations and fit are indicated.

concentrations ranging between 0.004-mg/ml to 0.100-mg/ml (Figure 15). Regression analysis was performed using Graphpad Prism to assess and define a linear relationship between absorbance and concentration values. The linear relationship was used to define calibration curves as it confirms the Beer-Lambert law was obeyed.

The shape of spectra profiles observed (Figure 14) over various concentrations were consistent in profile shapes with amplitudes varying proportionally to RIS concentrations. The calibration curve at 280-nm for RIS solution prepared over concentrations ranging between 0.004-mg/ml to 0.100-mg/ml was defined by the linear regression Equation 1 with an R^2 of 0.98.

$$\mathbf{Y_{280nm} = 3.75*(X) + 0.011}$$

Equation 3 Line equation of absorbance-concentration 280 nm

Linearity was thus confirmed and the Beer-Lambert law was obeyed (Equation 3).

The absorbance-concentration calibration curve at 315-nm was assessed over concentrations ranging between 0.75-mg/ml to 7.50-mg/ml. The calibration curve was defined by the linear regression Equation 2 with an R^2 of 0.98.

$$\mathbf{Y_{315nm} = 0.060*(X) – 0.015}$$

Equation 4 Line equation of absorbance-concentration 315-nm

A linear relationship was confirmed indicating that the Beer-Lambert law was obeyed (Equation 4).

UV/Vis analysis of samples collected from separately-prepared 5-mg/ml RIS solution batches were plotted on the absorbance-concentration calibration curve at a wavelength of 315-nm, indicated by the downwards arrow in Figure 15. The plotted 5-mg/ml RIS solution samples were qualitatively observed to be within range of the linear regression line corresponding with 5-mg/ml RIS concentration. Thus, the integrity and preparation of a 5-mg/ml RIS in solution was confirmed (Figure 15).

3.3.2 Risperidone Solution Pre-Formulation Stability Stress Test Results

Spectra profiles and measured sample concentrations were collected over multiple time points spanning 96-days. Samples were assessed and compared to

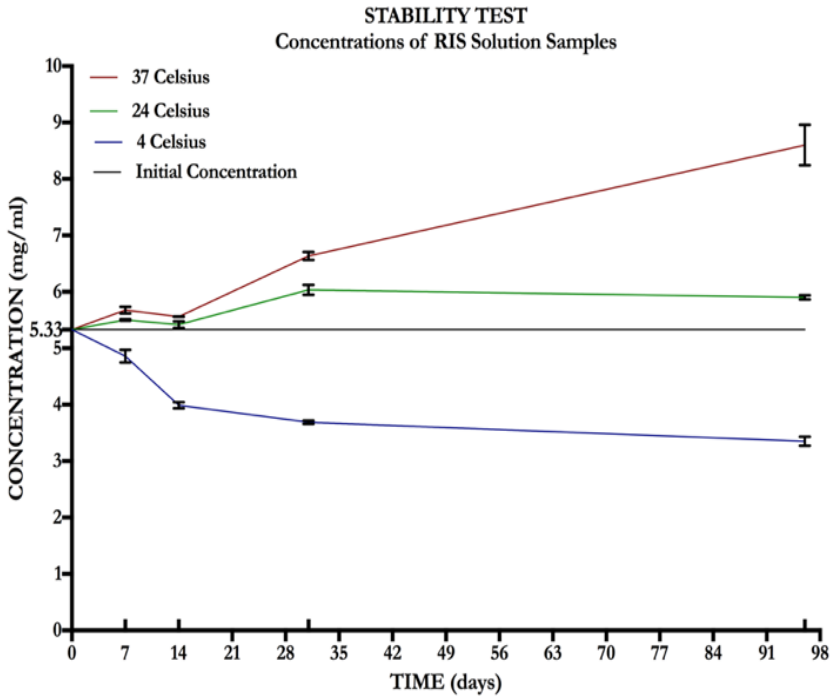

Figure 16 RIS solution concentration over time for samples stored at 4C, 24C, 37C over 96 days

the same measures collected on day-0 of the freshly prepared batch RIS solution, which was defined as the control measures (spectra profile and concentration). RIS solution was prepared at a concentration of 5.0-mg/ml, UV/Vis calculations quantified the prepared RIS batch solution at a concentration of 5.3-mg/ml. Each time point graphed in Figure 16, shows the average concentration measure and

respective standard deviation quantified based on an n = 3 of RIS solution vials at each temperature condition (or 9 vials of RIS sample solutions, plus 3 formulation vehicle solution samples at 0 mg/ml stored at each temperature condition). The concentration of RIS solution was compared to the initial sample collected from the batch 5-mg/ml RIS solution prepared on day-0. Concentration calculations corresponding with results graphed in Figure 16, are also shown numerical in Table 4. Values for each storage condition are shown for the average concentration of RIS over the three samples, corresponding standard deviation, and the percent concentration change of RIS with respect to the control RIS concentration calculated from a sample of the batch preparation collected on day-0.

Stability was assessed by graphically comparing collected samples spectra profiles against that of the control. Samples were read using UV-Vis and concentrations were calculated using the absorbance-concentration calibration curve at 315-nm wavelength, defined above in (Equation 4).

	4 C			24 C			37 C		
# OF DAYS	Mean	SD	% Change C_0	Mean	SD	% Change C_0	Mean	SD	% Change C_0
0	Initial Concentration (24 C) = 5.33 mg/ml								
7	4.86	0.11	8.85	5.50	0.01	3.20	5.68	0.06	6.42
14	3.99	0.06	25.22	5.42	0.06	1.60	5.56	0.01	4.22
31	3.69	0.03	30.81	6.03	0.09	13.15	6.64	0.07	24.45
96	3.35	0.08	37.16	5.90	0.04	10.70	8.60	0.36	61.32

Table 4 Stability test results showing concentration of RIS solution samples as an average of 3 samples, standard deviation, and percent change from initial RIS solution concentration over time with respect to storage temperature conditions

3.3.2.1 Stability of RIS solution stored at 4 Celsius over 96 days

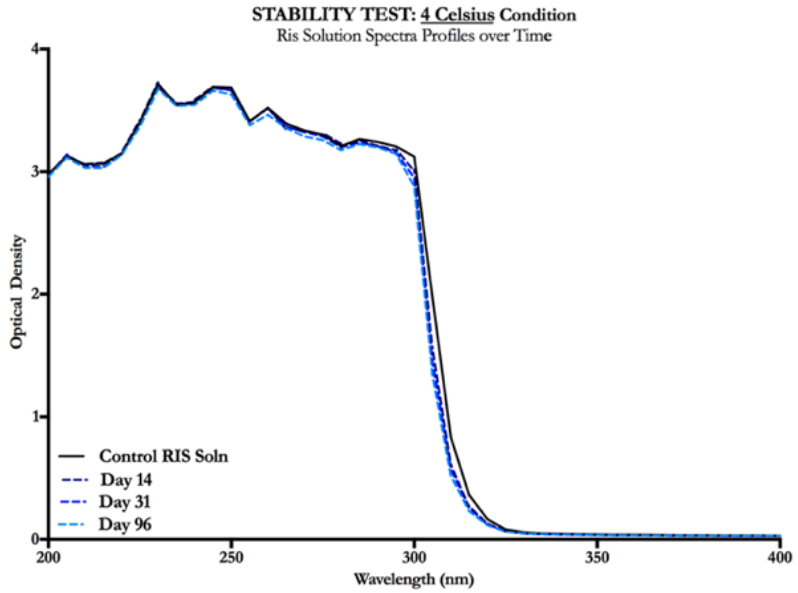

Figure 17 Stability stress test of RIS solution over time stored at 4C, spectra profiles of sample collection on days 0, 14, 31, and 96.

The spectral profile of RIS in solution stored at 4°C over time (Figure 17) remained consistent with the control spectra profile shape taken on day 0 of freshly prepared batch 5-mg/ml RIS solution. Spectra profile amplitudes were observed to have a slight downward shift along the Y-axis, which corresponds with a drop in RIS concentration.

Generally, the solubility of RIS in the prepared solution was observed to decrease with decreasing temperatures. Samples stored at 4°C indicated decreasing concentrations of RIS over time. By day-14, RIS concentrations decreased by more than 25% and by more than 37% on day 96 as compared to the control RIS solution. The concentration of RIS in solution stored at 4°C showed a

decreasing trend. The decreasing concentration of RIS in solution trend over time is hypothesized to be the result of RIS drug precipitating out of solution over time. The hypothesis of precipitation is supported by the change in RIS concentration as compared to the control over time leveling off after a period between 14-days to 31-days, after which the RIS concentration remains consistent. Based on these results RIS solubility decreases with decreasing temperatures.

3.3.2.2 Stability of RIS solution stored at 37 Celsius over 96 days

The stability of RIS solution stored at 37°C were analyzed. The elevated storage temperature over time resulted in the spectral profile shape deviating from the control on day-0. On the 96^{th}-day, spectra shape indicates the formation of a new absorbance peak within 300 – 400-nm wavelength range. The peak formation indicates the formation of a newly developed chemical entity which is the resulting degradation product of the initial chemical compound.

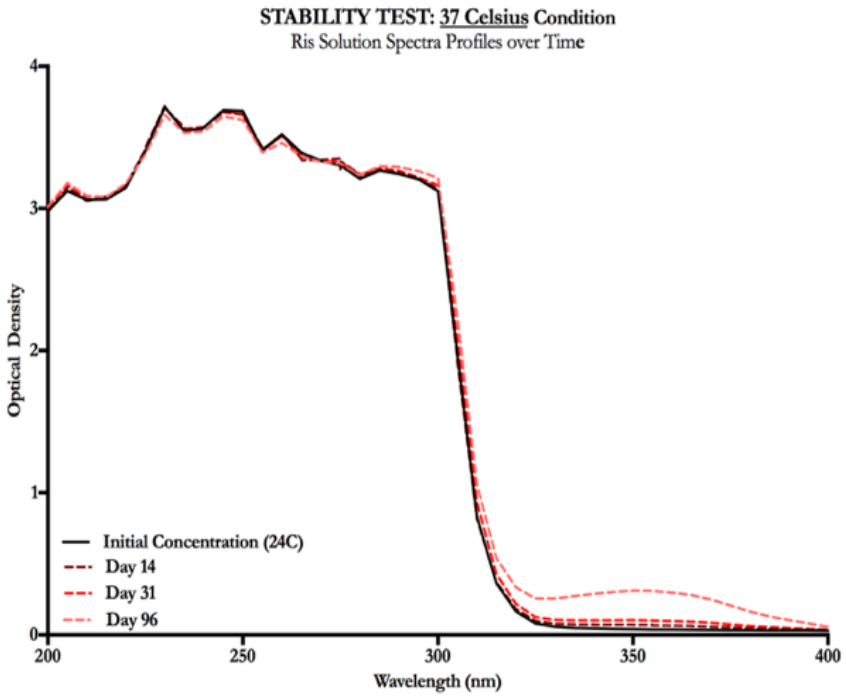

Figure 18 Spectra profiles over time of samples stored at 37C compared with control

The degradation of RIS solution samples stored at high temperatures were also represented in the concentration-time deviations of collected samples. On day-14, samples stored at 37°C had an average concentration that was within 10% of the initial control sample concentration (5.3-mg/ml). However concentrations of RIS samples evaluated and collected on day-96 had an average deviation of >60% from the base control RIS concentration measured on day-0. The concentrations of RIS stored at higher temperatures increased in concentration over time with respect to the control baseline sample concentration measures.

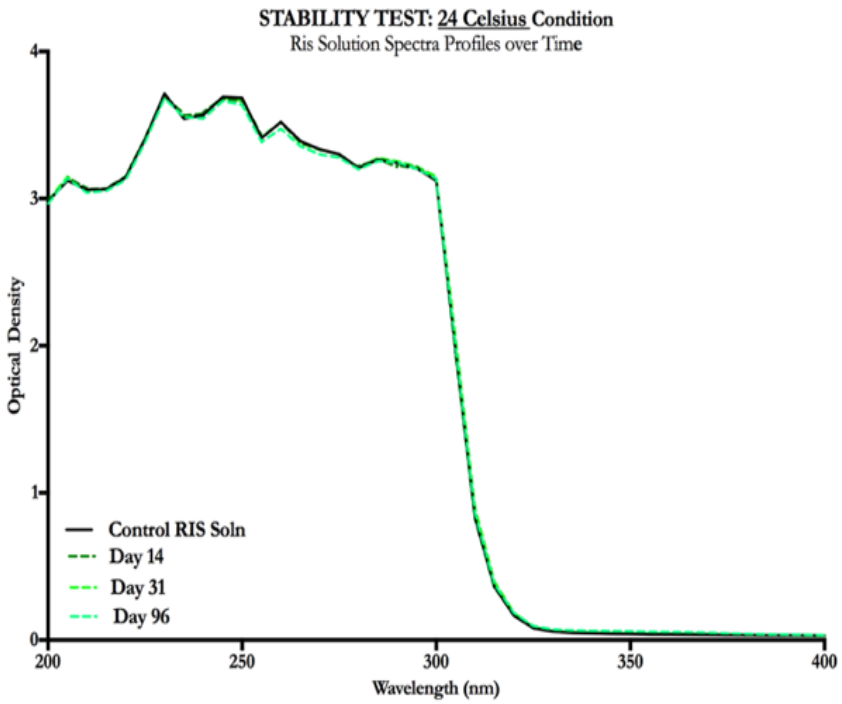

Figure 19 Spectra profiles over time of samples stored at 24C compared with control

The increase in RIS concentrations in prepared solution stored at high temperatures was hypothesized to likely be the result of evaporation of the liquid excipients namely H_2O and EtOH, or the confounding contribution of the new peak formation.

3.3.2.3 Stability of RIS solution stored at 24 Celsius over 96 days

RIS solution stored at 24°C was confirmed to be stable. The profiles over time were observably consistent in shape to that of the initial batch preparation or the control sample profile. Samples were without any indication of a new peak

absorbance formation which would indicate the formation of a degradation product.

The concentration of RIS in solution increased through Day-31, which is likely due to evaporation of the solution base or vehicle (25% PG: 25% EtOH: 50% H_2O) but stabilized thereafter. Oscillations in the concentrations stored at 24°Ccould be explained by RIS dissolving/precipitating in and out of solution. Additionally, fluctuations in the (room) temperature of the storage environment is possible given a larger space and a less controlled environment.

3.3.2.4 Stability of solution base without RIS over time and different temperatures

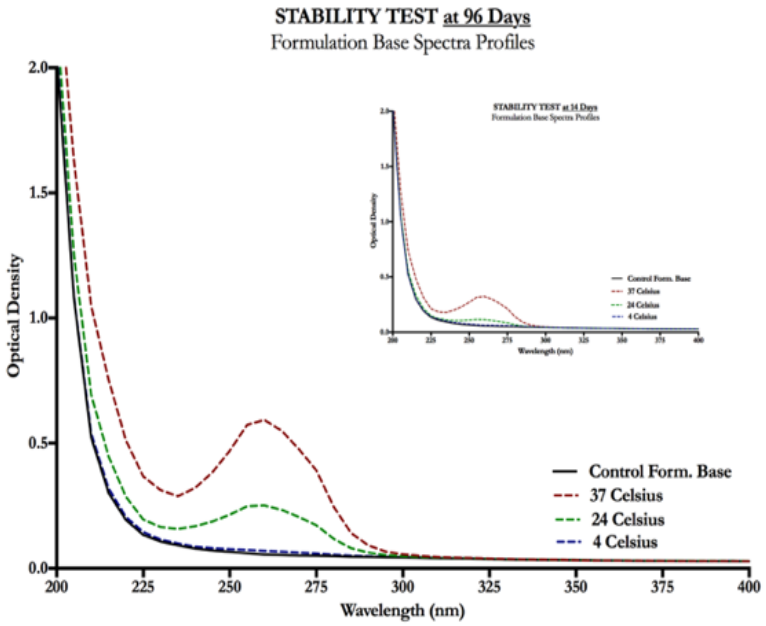

Figure 20 Spectra profiles of solution base without RIS over time of samples stored at 4°C, 24°C, 37°C compared with control

The spectral profile of the formulation base sample stored at 4°C remained consistent with the control (Figure 19). At 24°C and more notably with the increase of storage temperature to 37°C, the formulation base spectral profile deviated from the control, with increased optical density/absorption observed across all wavelengths and peaking at 260-nm. Given the temperature correlation, the increased optical density observed at higher temperatures could be the result of polymerization of the Propylene Glycol. Alternately, the prepared formulation base batch may have been contaminated leading to its degradation over time.

In summary, a RIS solution at a concentration of 5 mg/ml was prepared using the following excipients FDA GRAS (safe) approved excipients for dissolution in the following volume percent ratios:

25% Propylene glycol : 25% Ethanol (95% v/v) : 50% Water (%v/v/v)

The described solution of RIS was confirmed to be viable for the experimental objective and purpose of this paper. The 5-mg/ml RIS concentration was estimated to have an acceptably optimized concentration able to theoretically meet the required therapeutically-relevant deep lung delivered dose ($\leq$ 2-3 micrometers). The theoretical estimation was evaluated based on drug to the delivery device in the form of dead volume to the delivery device as well as the deposition of aerosolized drug within the pulmonary regions not associated with systemic uptake (emitted drug particles with aerodynamic diameters greater than 3-μm and less than 0.4-μm) (50).

The stability of Risperidone (RIS) at a concentration of 5-mg/ml within the above defined preparation was determined to be stable and safe when stored at room temperature conditions (24°C) for the experimental purposes here within. The concentration of Risperidone prepared at a concentration of 5-mg/ml in solution, was assessed for its ability to meet the 1-mg delivered dose criteria given drug-losses to the delivery device and route. The 5-mg/ml RIS solution concentration was found to be theoretically feasible in achieving the determined

deep lung delivered dose of 1-mg Risperidone for therapeutically-relevant treatment. This will be presented and explored in the following chapters.

In addition, the solution excipients utilized to prepare the RIS solution were GRAS (generally recognized as safe) approved by the FDA for a solution to be aerosolized for the pulmonary delivery of a pharmaceutical agent. These results meet the feasibility criteria outlined in Table 1.

3.3.3 Limitations & Future Considerations

The solution base or vehicle when stored over time, specifically at time point of >31-days, stored at temperatures of 24°C and 37°C, showed signs of chemical degradation. The degradation product formation is indication by the appearance of a previously non-existent peak formation based on the absorbance (optical density) – wavelength from UV/Vis readings. The degradation product could be the results of polymerization or indicate the presence of a contaminating product. Further testing is required to better understand the reason for the presenting degradation product. The degradation product might not impact the integrity of the drug solubilized in the solution excipients, however this has yet to be determined. This requires better understanding through further exploration and evaluation. Importantly, the degradation occurs only in the formulation buffer solution samples and not due to the resulting presence of RIS.

The stability of 5-mg/ml RIS solution stored at room temperature was appropriate for experimental purposes. However, for clinical application at least 1-year shelf-life indicating drug stability is required. Further testing is thus

required of the above pre-formulation development of RIS solution. Given the stability test results it is likely that adjustments within the described solution might be necessary for further stability development should it be pursued for clinically oriented applications.

Pre-formulation development might consider substituting ethanol with methanol for comparison and de-ionized H_2O with distilled water for an easily viable comparison. Slight adjustments to the pH of the solution for stabilizing Risperidone is a simple adjustment that could offer potential benefit. pH adjustments must remain within a safe range for the pulmonary administration route, as the lungs are a highly (pH) sensitive environment. While pulmonary environment is pH neutral, there is some room for mild pH adjustments to the solution.

3.4 CONCLUSION

A 5-mg/ml RIS solution was described and analyzed in the above Chapter 3. The solution excipients were FDA GRAS approved in the following - 25%:25%:50% (vol/vol/vol) ratio. The stability of a 5-mg/ml RIS solution was stress tested under various conditions (temperature, time), and the drug was found to be the (most) stable at 24ºC, or room temperature. The solution concentration changes with the storage temperature: increases with increased temperature, and decreases with decreased temperature. The concentration of 5-mg/ml RIS in

solution was considered appropriately high for achieving desired aerosolized deep lung dose.

4. AEROSOL CHARACTERIZATION RISPERIDONE & JET NEBULIZER (PARI LC®)

The PRE-formulation results were appropriate for the desired application - to experimentally aerosolize a RIS loaded solution, characterize the emitted aerosol, and utilize the results to assess the technical feasibility of using the pulmonary delivery route for the treatment of schizophrenia. The 5-mg/ml RIS solution will be assessed for its ability to adequately function with a jet nebulizer to produce and emit aerosol loaded with drug. This will be measured by determining the volumetric flow rate emitted from the nebulizer's output nozzle (Chapter 5). The stability of aerosolized Risperidone by the selected representative delivery devices, specifically the jet nebulizer given it is extensive use while being FDA approved and regulated, will be assessed (Chapter 5,6). The volumetric flow rate and emitted aerosolized drug stability are significant criteria in the evaluation of technical feasibility. Given the flow rate of emitted aerosolized drug is adequate and its stability confirms it as safe, aerosol characterization experiments utilizing the 8-stage Anderson Cascade Impactor will be developed and performed.

In chapter 2, an optimal dosing regimen delivered to the deep lung, region of the lung associated with systemic uptake, was determined to be a 1-mg RIS dose administered every 12-hours. A 5-mg/ml RIS solution was described in Chapter 3 and met the outlined feasibility criteria given the experimental purpose here within: FDA approved safe excipients, stable or safe stored at room

temperature over time, and drug concentration was deemed reasonable for achieving the deep lung delivered dose determined in Chapter 2.

The 5 mg/ml RIS solution (defined in Chapter 3) – jet nebulizer (PARI LC®) was evaluated for functionality as it pertains to producing and emitting aerosol: an adequate emitted volumetric flow rate supports further feasibility exploration to determine if aerosolized RIS by jet nebulization is stable (remains pharmaceutically relevant without new chemical products) based on UV/Vis spectral profile shape (refer to previous Chapter 3 for stability assessment methods). Subsequently, aerosolized RIS was characterized based on the aerodynamic particle diameter distribution which was quantified and analyzed using an 8-stage Anderson cascade impactor (ACI). Aerosol characterizing parameters were calculated and the technical feasibility of delivering a deep-lung systemically-available dose of RIS was assessed for its therapeutic relevance. The administration criteria for achieving therapeutic exposure and effect was criteria used in the assessment of technical feasibility.

4.1. INTRODUCTION

The following experiments used a jet nebulizer (PARI LC®)to aerosolize the developed RIS solution (Chapter 2) and preliminarily assesses the feasibility of systemically delivering RIS by inhaled administration. Pulmonary delivery offers unique advantages over the alternative oral (standard of care) and injectable

(long –acting) administration options. The pulmonary route for systemic delivery offers rapid drug absorption into the bloodstream resulting in similar pharmacological profiles to that of IV bolus injection[1] (63). In contrast to an IV bolus injections, inhalation is self-administered and not associated to the same degree with discomfort or pain (29).

Compared to orally ingested drug administration, the lung presents a low-enzyme environment that is void of hepatic first pass metabolism. During oral administration, a drug is absorbed by the digestive system then into the liver prior to entering systemic circulation for delivery. Enzymes function to catalyze metabolic processes, which is central to the function of the hepatic and digestive systems. Enzymatic presence decreases the administered dose or amount of drug available for delivery because of drug metabolism prior to its systemic absorption referred to as first pass metabolism or effect. Enzymes are present most significantly in the liver, the gastrointestinal tract and gut wall of the digestive system, which results in significant drug loss of orally administered drug. RIS tablets (standard of care) for example have a 60% bioavailability compared to the 100% bioavailability of an intravenous injections (86).

To achieve inhaled systemic drug delivery, the emitted aerosolized drug (RIS) must have a sufficient dose delivered within the aerodynamic particle diameter (APD) size range of less than 2 to 3 micrometers. In Chapter 2, it was determined that the optimal deep lung delivered dose (APD < 2-3 microns) of RIS

to achieve therapeutically relevant exposure-effect profile for the treating the symptomology associated with schizophrenia. This deep lung delivered therapeutically-relevant treatment dose was determined to be 1-mg.

First the stability of aerosolized RIS produced by a jet nebulizer was evaluated. Given drug stability was confirmed, delivering an aerosolized deep lung 1-mg dose of RIS (<2-3 microns) was technically assessed using an 8-stage ACI for its feasibility(50). The aerodynamic particle diameter size range of less than the following range of two to three micrometers is associated with drug particle deposition in lung regions associated with systemic uptake or the deep lung(50).

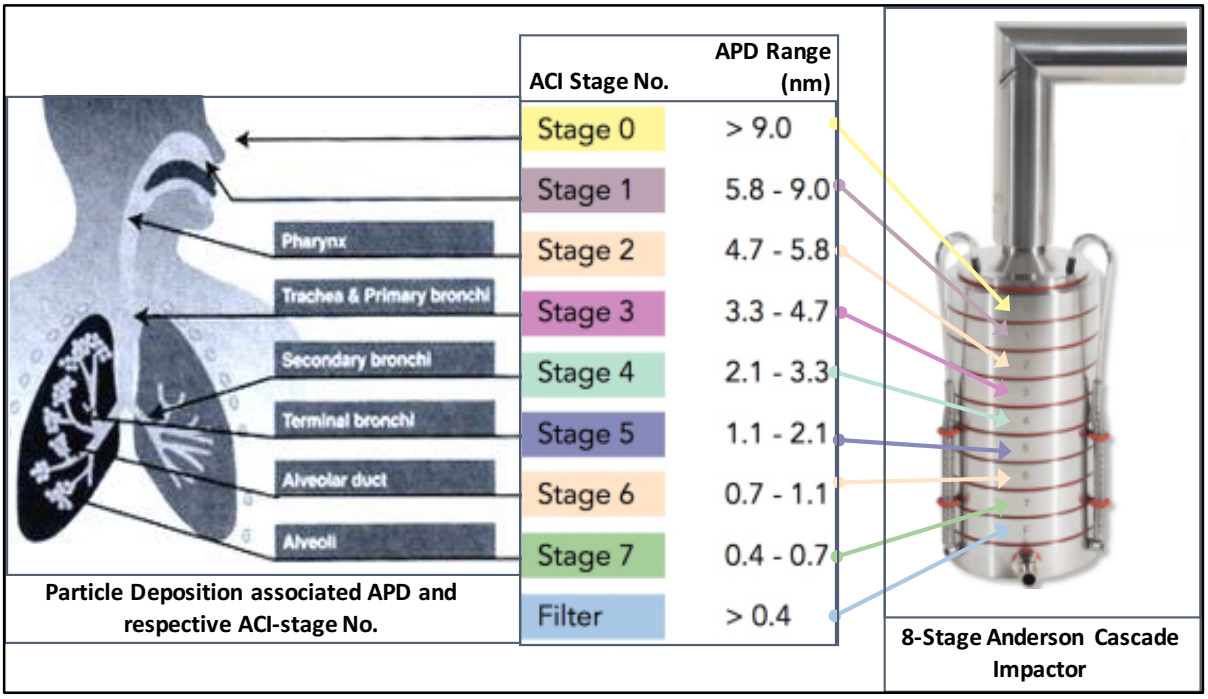

Figure 21 aerodynamic particle diameter band ranges associated with deposition within the pulmonary route and its relationship with ACI stages

An eight-stage Anderson Cascade Impactor (ACI) and a 28.3 - L/min suction pump with a constant flow rate, was used to capture and gather emitted aerosolized RIS particles for data collection and analysis. The ACI is an FDA approved laboratory device for gathering pre-clinical pharmaceutical aerosol data for characterization and analysis. Conclusions were based on the aerosolized drug's APD and the corresponding pulmonary region of deposition (87).

The ACI uses particle inertia, a function of both velocity and aerodynamic particle diameter, to separate and section aerosolized particles into separate stages by aerodynamic particle size bands (Figure 21). The stages' discrete aerodynamic particle diameter band ranges are associated with regions of the respiratory tract wherein aerosolized drug deposition is likely to occur. The stages contain

precisely engineered nozzles, each stage distinct in nozzle size and number. A frictionless plate follows each stage such that the airstream of drug-laden aerosol flows around the plates' circumference. As the aerosol moves progressively further through the ACI, the airstream's velocity increases as the diameter and the number of nozzles decrease and increase respectively. Drug particulates with sufficient inertia and an aerodynamic particle size within the stage's predicated band range will fall out of the airstream and deposit onto the stage's corresponding plate (stage-plate). Drug particle with an aerodynamic diameter smaller than the stage's size range will have an insufficient inertia, remaining entrained in the airstream to subsequent stages in the ACI. Drug particulates will stay in an airstream until its aerodynamic diameter falls within a stage's band range where sufficient particle inertia will result in its deposition.

The aerodynamic particle size bands that corresponds with an eight-stage ACI and a 28.3-L/min flow rate are shown in Figure 21. The effective stage cut-off diameters (ECD) with this experimental set-up correspond with those shown in Figure 21. The following experiments describe particles on plates 3 - 7 (4.7 - 0.4-μm) as inhalable. The delivered dose was defined as mass sum of aerosolized drug particulates within the aerodynamic particle diameter range of 0.4-micrometers to 3-micrometers (50, 87, 88).

Aerosol characteristics are a function of the combined delivery unit comprised of the drug's formulation and device selected. Here within the 5-mg/ml

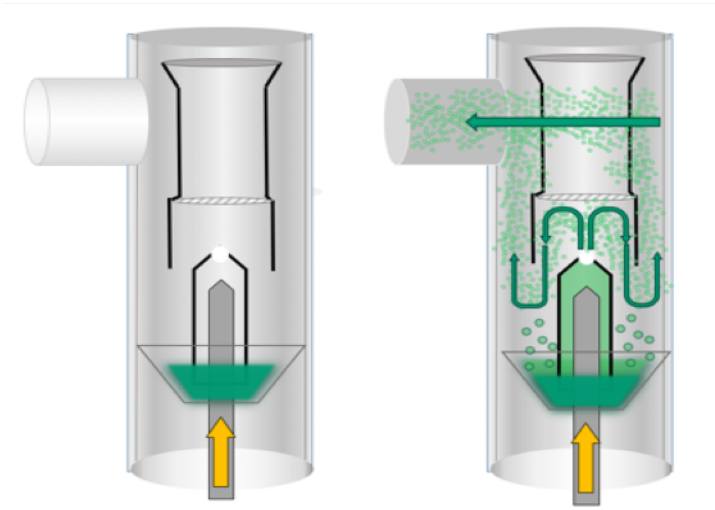

Figure 22 Depiction of the flow process and functionality of a basic jet nebulizer. Yellow arrow from the bottom point up indicates the attached compressor generating airflow up through the baffle. The green arrows just the path of the airflow through the solution to form aerosol.

RIS solution described previously in Chapter 3 was aerosolized using a PARI-LC(^{td}) disposable jet nebulizer.

A jet nebulizer functions (see Figure 22) through the force of a high-pressure system that passes compressed air into the nebulizer cup (contains drug-loaded solution) via a narrow tube and small outlet. When the constrained air enters the nebulizer, its velocity increases and results in a negative pressure at the outlet's point. The drug-loaded solution is drawn through narrow channels at the center of the nebulizer towards this region of negative pressure (Bernoulli Effect). The solution is drawn into the high velocity airflow where it is sheared into fine and unstable liquid films. Surface tension forces cause these unstable films to

break into droplets. A baffle physically inhibits larger droplets from exiting the nebulizer and helps to regulate the sizes of the emitted particles (89, 90).

The stability of aerosolized RIS was evaluated to determine the safety and pharmacological integrity of the delivered drug. Aerosol characterization was based on the aerodynamic particle diameter distribution (APDD) of emitted RIS deposition within the ACI. The aerodynamic particle diameter distribution was used to determine the mass median aerodynamic diameter (MMAD) of aerosolized and emitted RIS particles as well as the geometric standard deviation (GSD) or spread of the aerodynamic diameters (AD). The emitted dose (ED) was defined as the mass sum of aerosolized drug that was emitted from the jet nebulizer and/or captured within the ACI (all components – stage, plates, adapter, filter).

The aerosol produced from the jet nebulizer - RIS formulation combined system was characterized by the analysis of the following parameters: drug mass-size distribution, emitted dose and respirable fraction/nebulizer efficiency, dose delivered (to deep lung available for systemic delivery) and inhalable dose fraction, mass median aerodynamic diameter and geometric standard deviation for statistical analysis, mass balance and percent drug recovery to assess experiment and system integrity (see Table 5). The system's feasibility was further evaluated for RIS' stability during nebulization and whether the aerosolized mass of respirable RIS, met or could potentially meet, the defined criteria (Chapter 2) of emitting a systemically delivered dose of 1-mg RIS or greater.

PARAMETER	DEFINITION	CALCULATION	EQUATION
Initial Dose	The total drug mass loaded into the delivery device prior to experimental runs	UV/Vis reading of soln absorbance @ 315-nm determined concentration and thus mass	**= Drug mass (UV/Vis @ 315-nm) * volume**
Aerosolized Dose	Total drug mass emitted during experimental runs from the delivery device into the ACI	Total drug mass calculated and summed in all ACI components	**= RIS mass (adapter + stage walls +stage plates+ filter paper + connector components)**
Emitted Dose (ED)	Total drug mass deposited on all plates in the ACI (0-7,F)	Samples collected from all plates were read with UV/Vis. Relevant calibration curve determined drug concentration	**= sum (each plate drug concentration * volume of solution base added to solubilize emitted drug particulates)**
Aerodynamic Particle Diameter Mass Distribution (ADPD)	The fraction of drug mass within each aerodynamic diameter particle size range of the ACI as a fraction of the total ED	Total sum of drug on each plate as a percent of total emitted dose plotted against the aerodynamic particle diameter range corresponding with the respective stage plate diameter range	**= (mass of drug per stage plate)/(ED**
Mass Median Aerodynamic Diameter (MMAD)	The aerodynamic particle diameter at 50% of the cumulative distribution wherein which 50% of total drug mass of the ED falls in the aerodynamic particle diameter range below he MMAD and 50% of ED drug mass is above	-Logarithmic – prohbit scale plot: Logarithm of effective cut-off diameter (ECD) given stage range vs. the inverse normal cumulative mass drug distribution with mean of 50 and std of 1 -Regression analysis to determine the best line fit (least squares)	**=linear regression was solved for at x= 50**
Geometric Standard Deviation (GSD)	The spread/deviation of aerodynamic diameter drug mass around the MMAD	Refer to MMAD calculations above	**= square root of (10^ linear regression equation @ x=51)/ (10^ linear regression equation at x= 49)**
Delivered Dose (systemic uptake)	The total mass of drug (<2-3 microns) with aerodynamic particle diameter in the range between 0.4 microns (filter) to 3 microns	Total sum drug mass of RIS within the aerodynamic diameter range 0.4-3 microns	**=std nrml dist (@ 3 microns, mean=MMAD, std dev=GSD, cum dist = true) – mass below 0.4 microns**

Table 5 Aerodynamic Characterizing Parameters Summarized

4.2 MATERIALS & METHODS

4.2.1 MATERIALS

RIS and Form vehicle, vacuum suction pump (28.3-L/min), 8-stage ACI Copley Scientific with cut-off diameter, UV Vis spectral scan & Corning 3635 - 96 well plate, UV-transparent, acrylic copolymer, flat bottom, clear, non-sterile, 50/cs - clear plates, Ziploc-style collection bags.

4.2.2 METHODS

ACI experiments were run with a prepared 5-mg/ml RIS formulation, previously described, composed of: 25% v/v propylene glycol, 25% v/v ethanol (95%), and 50% v/v purified water. The preliminary nebulizer tests were performed with a 7.5-mg/ml RIS formulation with the same composition and preparation. RIS concentration was determined using UV-Vis spectra and standard curve relationships discussed in Chapter 3. [wavelength 315-nm (0.75 – 7.50 mg/ml) and 280-nm (0.001 – 0.400 mg/ml)].

Prior to running each experiment, the prepared RIS formulation and its formulation base (without RIS) were sampled and UV/Vis spectra data was obtained as a control. After an experimental run was complete and aerosol production was stopped, the system was disassembled and additional samples were gathered. Samples were obtained using measured volumes of the formulation to extract, solubilize, and collect all RIS within the contained experimental system. Experimental data for all samples was obtained using UV Vis to generate spectra data in 5 nm increments between the wavelengths of 200 – 400 nm. UV/Vis spectra data was gathered with a UV-transparent 96-well plate containing samples that were 0.100-ml in volume. Spectra data was used to observe a sample's spectral profile (a plot of wavelength versus optical density) and to determine the concentration, and subsequent amount, of RIS.

As previously described in Chapter 3, the concentration of RIS was determined using the collected sample OD, and standard curve at the wavelength, of 315-nm.

Mass balance calculations were performed for all experiments to ensure a proper closed-system, experimental set-up. The mass of RIS was quantified at the beginning and at end of the experiment. The initial mass of RIS was defined as the RIS dose (or RIS formulation) loaded into the delivery device which was determined from the analysis of a sample. The mass of RIS in the system at the end of an experiment was determined by sampling and quantifying the mass of RIS for parts of the experimental set-up (including the delivery device) which had contact with aerosol or formulation, and taking their sum to achieve the value for the total amount of RIS. The two total mass values of RIS were compared to ensure mass balance.

The stability of RIS was assessed by comparing the spectra profiles of freshly prepared RIS formulation samples (controls) to those of collected samples'. RIS was deemed stable if the collected samples' profiles matched, in form and shape, to the freshly prepared samples' profiles. New peak formations not previously observed in the control profile shape indicates a new chemical compound formation resulting from the process of degradation.

Experiments were set-up as a closed system, and run in a ventilated hood with equipment that had been cleaned and dried: 70% ethanol was sprayed and removed from equipment by evaporation or with Kim wipes, followed by being immersed under continuously flowing warm water, subsequently all equipment was soaked in de-ionized water for approximately 12-hours before being air dried for a minimum period of 12-24 hours.

Prior to commencing each experiment, samples of the prepared RIS formulation and formulation alone were collected and UV/Vis spectra data was used to quantify its concentration and determine the mass of RIS contained in the initial dose. A precision scale was used to measure the mass of the delivery device.

The nebulizer's mass was taken prior to loading a 2-ml dose of RIS formulation (at 7.500-mg/ml) into its cup, after which another mass reading was

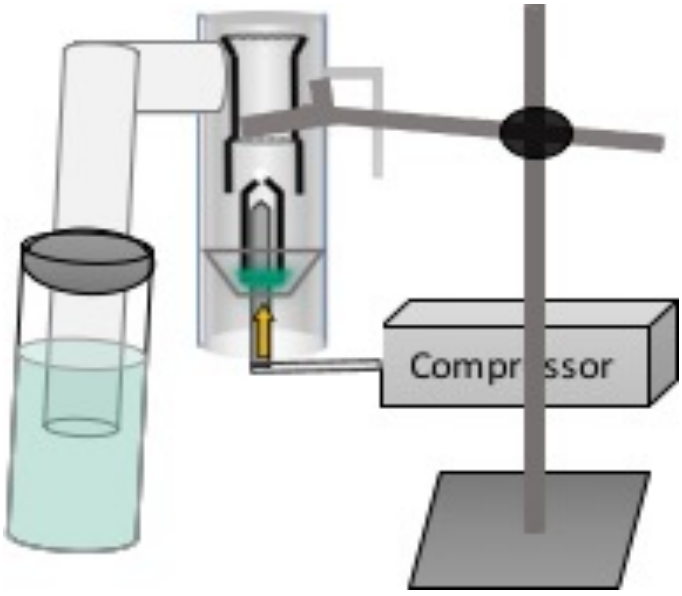

Figure 24 nebulizer and RIS solution testing without ACI for determining volumetric flow rate of emitted aerosol exiting from the output of the nebulizer

taken. tubing was used to connect the nebulizer, held upright and level by a stand, to the compressor (Figure 24). A 5-ml volume of the formulation was pipetted into a newly opened disposable plastic test tube (50-ml capacity). One end of a

plastic tube was fitted over the nebulizer's output and parafilm was used to seal the connection. The other end or opening of the plastic tube was submerged in the formulation in the test tube to entrap aerosol. The compressor was engaged for a timed period of 2-minutes and 30-seconds.

The system was disassembled and the nebulizer's mass was measured. The plastic tube was placed in a Ziploc-style plastic bag where its interior was rinsed with 1-ml of the formulation, which was then sampled along with the formulation test tube that was used to capture the nebulized aerosol. Samples

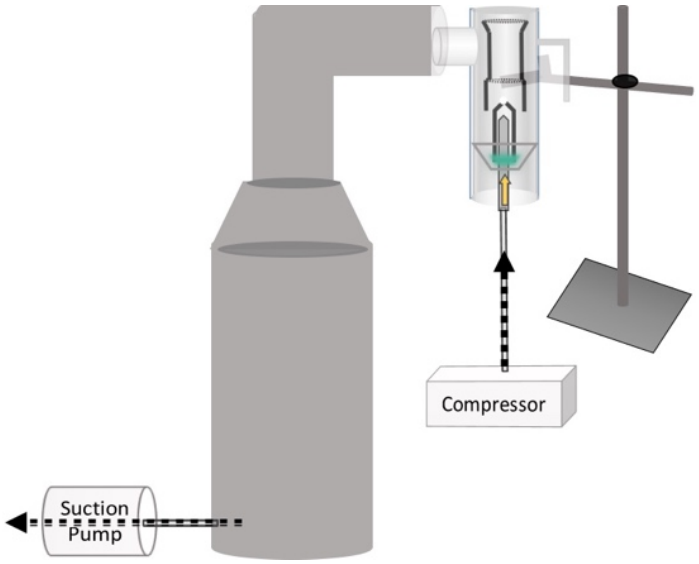

Figure 25 ACI and suction pump, jet nebulizer experimental set-up

were collected and observed as mentioned above at 315-nm. The data gathered was used to assess and determine the following parameters: the stability of RIS and the flow rate of aerosolized and emitted RIS.

The 8-stage Anderson Cascade Impactor (ACI) was assembled appropriately and attached to a 28.3-L/min suction pump. The ACI and suction pump were connected with tightly fitted plastic tubing. The ACI was used with a 0.22-micrometer filter paper following the final collection stage to capture RIS aerosol particulates/droplets with an aerodynamic diameter of < 0.4-μm and to maintain a closed-system. The nebulizer's mass was taken prior to loading a 3-ml dose of RIS formulation into its cup, after which another mass reading was taken. Provided tubing was used to connect the nebulizer, held upright and level by a stand, to the compressor. The stand was adjusted so the nebulizer's output was aligned, parallel and centered, to the ACI's input (Figure 25). The suction pump was engaged for 5-minutes prior to each experiment and disengaged when aerosol production was stopped. The compressor was engaged for a timed period of 5-minutes.

The ACI was detached from the tubing connected to the suction pump. The ACI was disassembled and all parts (21 in total) were separated into individual Ziploc-style closed plastic bags. The formulation was dispensed onto the bagged parts which were rubbed, wiped, shaken, and left to sit for 5 minutes. All items were sampled and treated as mentioned above. The volumes of formulation added to individually bagged ACI parts were determined based on the limit of detection associated with the absorbance-concentration calibration curve at 315-nm and ensuring an adequate volume was added to properly dissolve and collect all RIS deposition for sample collection and reading. General volumes of solution base added to ACI parts is shown in Table 6.

ACI Section	Volume of Formulation Base Used for Extraction (ml)
Neck	0.7-1
Throat	0.5
Filter Paper	N/A
Stage Walls (0-7, F)	0.6
Plates (0-7, F)	0.5-0.6

Table 6 Overview of solution base volumes added to individual ACI

A mass balance of RIS was performed for all experiments and the total drug recovery was reported to indicate experimental validity of system-up set-up, methodology, sample collection and quantification for subsequent analysis. The mass balance was calculated by finding the individual concentration of all individual ACI parts using the absorbance-concentration calibration curve at 315-nm (subtracting the solution base reading from the sample reading as mentioned previously). The resulting sample concentration was multiplied by the known volume of solution base or vehicle used to solubilize and collect RIS drug particle deposition. The nebulizer's residual RIS mass was calculated as previously described by way of mass change. The sum of RIS mass across entire system (ACI parts and nebulizer) was compared to the initial mass of RIS dispensed into the nebulizer cup. The initial dose of RIS mass was measured in the same manner as collected samples and multiplied by the volume pipetted into the nebulizer cup.

The total mass of RIS found in the ACI was calculated. The emitted dose of RIS was determined by taking the sum of RIS mass found over stage plates 0 – F. The aerodynamic particle diameter size distribution was graphed using the mass fraction of RIS on each plate over the emitted dose. The fine particle dose (FPD) was defined as the sum of RIS mass on stage plates 3 to F. The fine particle fraction (FPF) was calculated as the percent fraction of the fine particle dose over the total emitted dose.

The cumulative mass distribution of RIS particles on plates below the effective aerodynamic cut-off diameter of the above stage was determined. The cumulative distribution was plotted on a probit scale around the mean of 50% total mass on the x-axis and the Y-axis is the logarithm of the associated effective cut-off diameters of each stage. The log-probit scale plot was used for achieving a linear graphical relationship for analysis. Graphpad Prism was used to perform regression analysis and define the line equation(s). The line equation was used to determine the mass median aerodynamic particle diameter (MMAD) at 50% (x-axis). The MMAD is the aerodynamic particle diameter associated with 50% of the cumulative drug mass, such that sum of drug particles of aerodynamic diameter above and below the MMAD equates to 50% of the total emitted dose. The geometric standard deviation (GSD) describes the spread of emitted particles' aerodynamic diameters around the MMAD. The GSD was measured using the regression line equation, wherein the square root of the aerodynamic particle diameter ratios of 51% divided by 49% cumulative mass distribution was calculated.

4.3 RESULTS & DISCUSSION

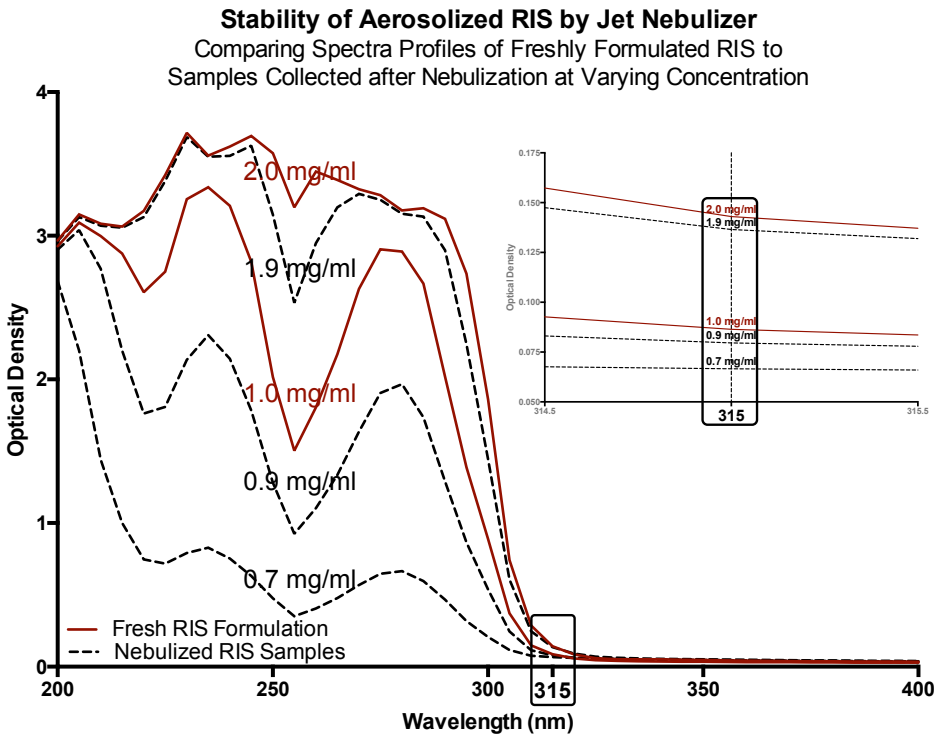

Figure 26 Comparing spectra profiles of aerosolized RIS by jet nebulizer to control samples for determining profile shape for stability

UV/Vis Spectra profiles of RIS solution prior to nebulization (determined in Chapter 3 freshly prepared samples and evaluated as controls) and post-nebulization are shown and compared in Figure 26; the samples are represented by a solid red line (controls profiles) and dashed-black line (aerosolized profiles).

The spectra profiles, pre-and post- nebulization, are similar in line shape. Spectra profile shapes collected from post-nebulized samples were absent of new peak formations. Peak formations indicate the presence of a chemical compound. New peak formations present within a spectral profile indicates the formation of a the formation of a degradation product based on the presence of new chemical entity formation.

The 5 mg/ml RIS solution preciously described was aerosolized by a jet nebulizer and results were assessed with UV/Vis. Based on the experimentally collected results and method of analysis, the pulmonary delivered dose of aerosolized RIS was found to be stable (suggesting safety). The safety of aerosolized RIS was determined based on UV/Vis spectral profiles of samples before and after aerosolization being consistent in line shape. Results indicated that RIS solution of freshly prepared sampled compared to samples from re-solubilized aerosolized RIS were consistent in spectra profile shapes. Thus the 5-mg/ml RIS solution aerosolized by a jet nebulizer remained safe. Safety was concluded from the stability and pharmacological integrity determined from the comparatively similar UV/Vis spectra profile results.

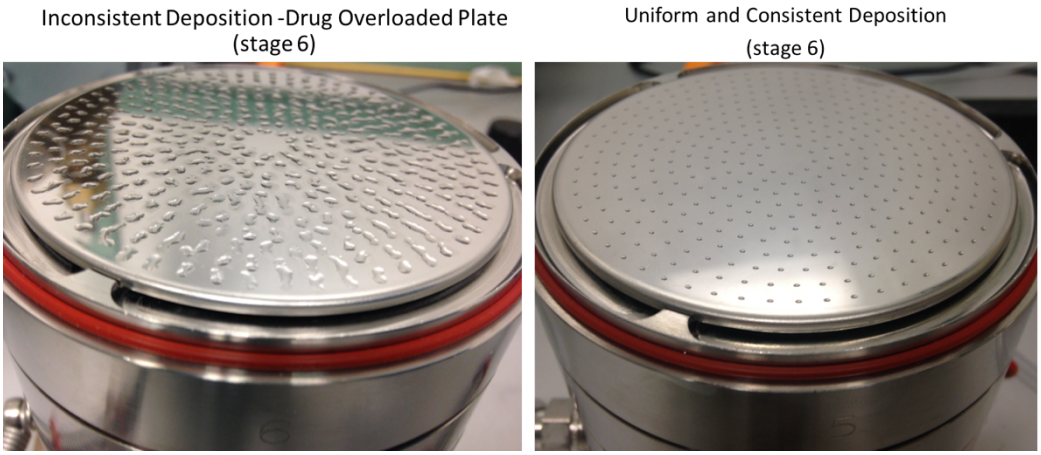

Figure 27 Example of experimental error vs to proper set-up: two Stage 6 plates are shown and compared for droplet deposition pattern and shape. Left image shows collected drug deposition show spattered and inconsistent in shape and distribution across the plate – the set-up is overloading the plate with drug which increases error. The Right image shows uniform and consistent deposition indicating that the experimental dosing (volume, time of aerosolization) is appropriate.

After experiments were run, plates were qualitatively assessed upon collection. Plates were observed to have drug particle deposition that was uniform in both deposition pattern and droplets were spherical in shape (see Figure 27), no signs of droplet splatter were observed for the reported experimental conditions. Based on these observations, the system set-up of nebulized RIS solution with respect to volume of aerosol emitted and time of nebulization showed no signs of overloading the ACI. Overloading the ACI leads to an increased chance of error(s). Inter-stage losses to the ACI walls accounted for 5.9% (+/-0.95%) of the total emitted dose of RIS collected on plates.

UV-Vis was confirmed as an appropriate method of sample quantification. All plate samples that were collected fell within the 315-nm absorbance – concentration calibration curve's limit of detection except for the filter paper and select stage walls, which fell below the detection limit. These readings were not included in the final results but did not have significant impact on results, which was concluded based on mass balance and the highly efficient recovery of RIS.

Experimental integrity was confirmed by way of mass balance and drug recovery, as well as result reproducibility. Mass balance was assessed and compared across the entire system (nebulizer and ACI) before and after experiment runs were performed. The total RIS mass recovered after each experiment was found to be >95% of the initial drug mass loaded into the nebulizer cup. ACI results of two runs, A & B, are shown in Figure 28 and Figure 30. Runs A & B had comparable results. In addition, quantitative results of relevant parameters were separately calculated for runs A & B (reported below).

The results for each run were similar. For example, aerosol-characterizing parameters for runs A & B were consistent with one another. Therefore, experimental methodology was validated: experimental set-up, sample collection, quantification, assessment and analysis of data. Subsequently, results were

considered representative of drug loaded aerosol that would be delivered to

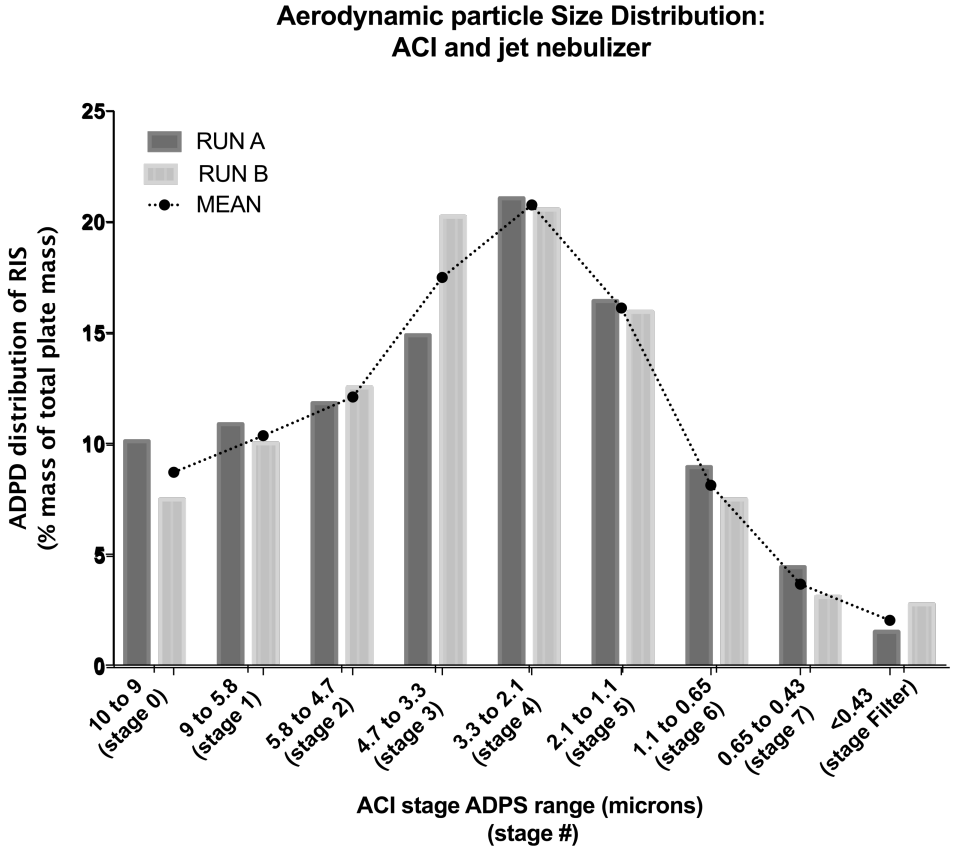

Figure 28 The aerodynamic particle diameter distribution of RIS as a percent fraction of the emitted dose

patients.

The PARI LC® nebulizer cup was loaded with a 3.0-ml volume of 5.0 mg/ml-RIS solution and continuously run over 5-minutes. The residual volume remaining in the nebulizer cup was based on mass change and found to be 1.2-ml and 1.0-ml for ACI runs A & B, respectively. The total mass of RIS aerosol deposited within the ACI (sum of RIS on all components: adapter, stage walls and plates, across 0 – 7 and F, including filter paper) for run A was 9.8-mg or 59.4% of the initially loaded dose RIS, and the same measures for run B was 10.6-mg or 61.5%. The emitted dose of RIS, defined as the sum of RIS mass on all plates (0-7, F) as a percent fraction of the total RIS mass calculated in the ACI was 88.4% and 85.6% for runs A & B respectively.

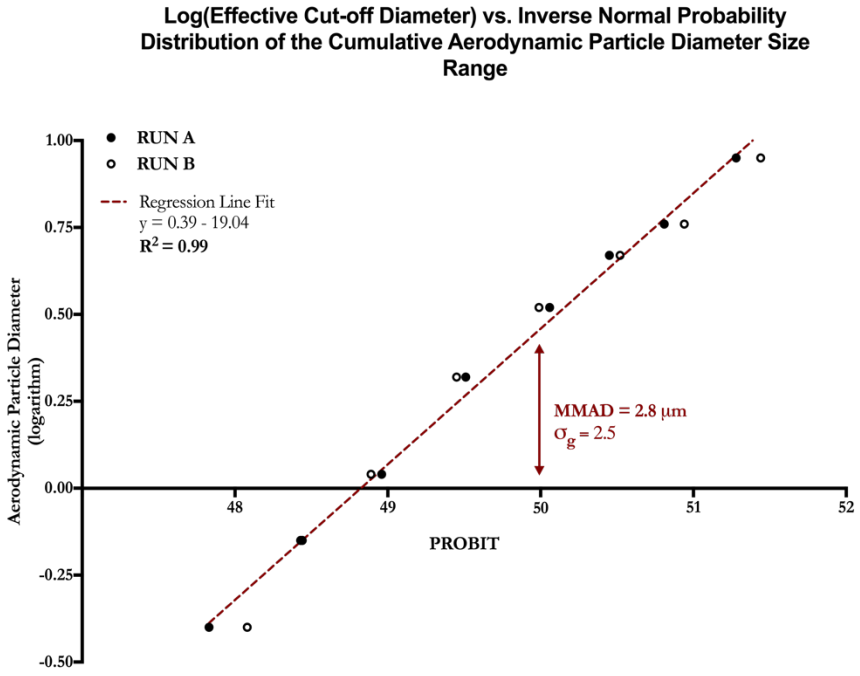

Figure 29 Regression Analysis and resulting MMAD and GSD calculations. Graph of log ECD and cumulative distribution on prohbit scale plot

The aerodynamic particle diameter distribution (APDD), shown in Figure 28, is presented as a bar plot. The APDD shows the mass of RIS on each stage plate (0-7, F) as a percent fraction of the total emitted dose (total mass on all plates) plotted against the associated aerodynamic particle diameter (APD) stage band range. The dotted-line plotted on the APDD shows the average of both runs (dot) for displaying the general distribution. The fine particle fraction (FPF) and fine particle dose (FPD) was defined as the mass sum of drug particulates with an aerodynamic particle diameter of less than 5-micrometers.

FPF and FPD were calculated as the mass sum of RIS deposited on stage plates 3 – 7, F (< 4.7 micrometers, sum of mass RIS deposited on stage plates: 3, 4, 5, 6, 7, F). FPF was reported as the percent fraction of the emitted dose defined as the mass of RIS on all stage plates. The FPF was the percent fraction of the sum of aerosolized RIS within the aerodynamic particle diameter size range region between 4.7 - 0.4 micrometers. FPF as a percent fraction of the total emitted RIS mass deposited and summed on all stage plates, was calculated to be 67.2% and 70.0% for Runs A & B respectively. The FPF measurements were based on the FPD (fine particle dose), and quantified as the total mass sum of RIS deposited on stage plates 3, 4, 5, 6, 7, and F. The FPD for Run A & B respectively was found to be 5.8-mg and 6.4-mg.

The ACI APDD results shown in Figure 28 were graphed and analyzed. The aerosol characterizing parameters, mass median aerodynamic diameter (MMAD) and geometric standard deviation (GSD), were calculated utilizing a line equation determined by regression analysis of plotted graphs of the

manipulated data: the logarithm of the lower effective cut-off diameter of each plate with respect to the inverse normal of the cumulative drug mass distribution below the corresponding effective cut-off diameter plotted on a prohbit scale (mean= 50, standard deviation=1).

The cumulative distribution of RIS mass on each stage plate below the effective cut-off aerodynamic diameter (ECD) of the previous stage as a percent fraction of the total emitted RIS dose is shown in Figure 30. The cumulative distribution of RIS mass in Figure 30, is graphed on a logarithmic-probit scale plot. The logarithm was taken of each stages' lower effective cut-off diameter (ECD) limit was calculated for the Y-axis data set. The corresponding cumulative mass distribution of RIS mass below the lower limit of the effective cut-off diameter of the previous stage (going from stage F – 100% cumulative mass to stage to stage-0) Ego-C® as calculated as a fraction of the total emitted dose (on all stage plates). The normal inverse of the cumulative mass distribution of RIS mass was quantified (mean of 50 (%) and standard deviation of 1). The logarithm of the lower effective cut-off diameter limits (Y-axis) was graphed against the associated cumulative mass distribution (x-axis) on a probit scale plot.

Runs A & B were graphed together. A regression analysis was performed (GraphPad Prism) for the combined data of runs A & B. Runs A & B were separately assessed however a combined model was found to be the best model fit for the data acquired. The regression fit had an R^2 of 0.99 and the line equation is shown below in Equation 5.

$$Y=0.39x-19.04$$

Equation 5 Line equation from regression analysis

Equation 5 was used to determine the mass median aerodynamic diameter (MMAD) and the geometric standard deviation (GSD), aerosol characterizing parameters. The MMAD was defined as the aerodynamic particle diameter of RIS associated with the 50% cumulative RIS mass distribution. The MMAD was calculated using the regression line equation, which was found to be 2.88-micrometers. The APD range for systemic uptake, deep lung drug delivery, is less than or equal to 2-3 micrometers (50). Results support initial technical feasibility based on the delivered dose (APD of <2-3 micrometers, associated with systemic uptake) representing 50% of the total emitted dose.

The GSD represents the spread of the emitted drugs aerodynamic particle diameter spread around the MMAD with respect to its cumulative mass distribution. The GSD was calculated to be 2.54, which indicates emitted a heterogeneous aerodynamic particle diameter size distribution . A heterogeneous aerodynamic particle diameter distribution is typical of a jet nebulizer (91). Results of these experiments are shown Figure 28 and Figure 30.

The average volumetric flow rate was determined based on initial nebulizer experiments not using the ACI. These experiments indicated an average volumetric flow rate of 0.35 –ml/min (SD). This volumetric flow rate was relatively consistent with the volumetric flow rate found for ACI based experiments

The total delivered dose of RIS was defined as the mass sum of aerosolized drug particles above 0.4-micrometers (filter stage) and less than 3-micrometerse, the literature suggests an aerodynamic diameter range of less than 2-3-µm (50). The total delivered dose between 0.4-micrometers to 3-micrometers was 4.42-mg. The delivered dose was founded based on experimental set-up of continuous nebulization over time. Based on the respiratory cycle having 50:50 inhalation to expiration ration, the delivered dose based on the above 5-minute administration time would be 2.2-mg.

4.4 CONCLUSION

The delivered dose was determined to be 2.2-mg based on a respiratory cycle of healthy individuals approximated as 50:50 inhaled to exhaled time ratio. Experiment results were representative of the dose delivered to individuals based on the stability and mass balance results. The delivered dose of 2.2-mg over the period of nebulization, exceeds that the required optimal 1-mg delivered dose for achieving therapeutically relevant effect. Feasibility was confirmed based on the pre-clinically relevant technical assessment described and reported on in the above chapter.

5. AEROSOL CHARACTERIZATION: ELECTRONIC CIGARETTE

The technical feasibility of a therapeutically relevant dose (1-mg) of RIS to the deep lung region using jet nebulizer as a delivery device was confirmed previously in Chapter 4. However, the jet nebulizers' form and function does not simulate the behavior associated with smoking a cigarette. While the pulmonary route for systemic drug delivery offers unique advantages mentioned in the initial introduction, an overarching goal was to validate a means to target low medication adherence rates associated with the target population of individuals with schizophrenia. Low adherence rates within this population are associated with numerous factors (see Introduction) with adherence being dependent upon patients' acceptance of related treatment(s). The same target population presents with comparatively high rates of smoking (tobacco) against the general population. Smoking or inhalation offers a familiar delivery route that is perceived as acceptable by the population of interest. Targeting habit-formed behavior has several other advantages (Introduction). The electronic cigarette as a delivery device has unique implications for clinical applications as an exploratory platform and diverse range of features possible, i.e. a platform upon which to better measure patient adherence given its easily programmable microchips.

5.1 INTRODUCTION:

Among psychiatric disorders, Schizophrenia, is associated with the lowest rate of treatment adherence leading to complications such as: increased relapse rates, more frequent hospitalizations, higher levels of treatment-refractory residual

symptoms and poorer long-term functioning and overall outcomes (4, 7, 92, 93). Smoking (cigarettes) is an intractable clinical feature of schizophrenia with its prevalence ranging from 70% - 90%, in stark contrast with roughly 20% of the American population smoking cigarettes (21,22). In addition, smoking is a highly-engrained behavior that is driven by neural changes induced by the repetitive nature of addiction.

Considering this, administering antipsychotic medications by inhalation may be associated with increased acceptability and adherence in this population. Given the above, a drug delivery device that is analogous to a cigarette may be therapeutically relevant, and have implicit value to this patient population. For this reason, an electronic cigarette was selected to assess the technical feasibility of delivering RIS by inhalation. In addition, an electronic cigarette provides a technically different delivery platform than the previously assessed jet nebulizer (Chapter 4) while accepting the same liquid formulation of RIS. As a well-established FDA regulated therapeutic device, the jet nebulizer was used in previous experiments to define and demonstrate the technical feasibility of delivering RIS by inhalation (Chapter 4). The electronic cigarette was evaluated, and experiments were run, with the same methodologies that were used for the jet nebulizer in Chapter 4.

Models and styles of electronic cigarettes (e-cigs) vary but they are functionally similar in their method of aerosol or vapor production. Liquid solutions of nicotine (or non-nicotine) for the e-cig are made from combinations of propylene glycol and/or vegetable glycerin with added flavoring. The cartridge

contains the nicotine solution that is fed to the atomizer, by a fiber or mesh wick, for vaporization by a material wick. The atomizer, comprised of a metal coil or heating element, vaporizes the nicotine solution from energy drawn from its battery connection. Vapor is emitted and inhaled by the user through the cartridge. Small airway inlets at the base of the atomizer and near the mouthpiece utilize inhalation to produce an airflow and changing pressure gradients. Airflow is drawn across and up through the heating element towards the mouthpiece for inhalation. Airflow also helps draw the nicotine solution down towards the

Figure 31 Comparing sizes of typical electronic cigarette device (Joye tech eGO-C® and CC®-roll) vs a cigarette (top image), (bottom image) depicts the general anatomy of electronic cigarette parts.

heating element for vaporization.

5.2 MATERIALS & METHODS

5.2.1 MATERIALS

A 5-mg/ml RIS solution (Chapter 3), vacuum suction pump (28.3 L/min), 8-stage ACI Copley Scientific with cut-off diameter, UV/Vis, Corning 3635 - 96 well plate | UV-transparent | acrylic copolymer flat bottom clear non-sterile 0/cs - clear plates, Ziploc-style collection bags. E-cig used was purchased as an advertised Joyetech eGO-C® device - atomizer, cartridges, battery.

5.2.2 METHODS

Experiments were run with a prepared 5-mg/ml RIS formulation, previously described, composed of: 25% v/v propylene glycol, 25% v/v ethanol (95%), and 50% v/v purified water. RIS concentration was determined using UV-Vis spectra and standard curve relationships discussed in Chapter 2 [wavelength 315 nm (0.75 – 7.5 mg/ml) and 280 nm (0.001 – 0.4 mg/ml)].

Prior to running each experiment, the prepared RIS formulation and its formulation (without RIS) were sampled and UV/Vis spectra data was obtained as a control. After an experimental run was complete and aerosol production was stopped, the system was disassembled and additional samples were gathered. Samples were obtained using measured volumes of the formulation to extract, solubilize, and collect all RIS within the contained experimental system. Experimental data for all samples was obtained using UV/Vis to generate spectra data in 5-nm increments between the wavelengths of 200-nm to 400-nm. UV/Vis

spectra data was gathered with a UV-transparent 96-well plate containing samples that were 0.1-ml in volume. Spectra data was used to observe a sample's spectral profile (a plot of wavelength versus optical density) and to determine the concentration, and subsequent amount, of RIS.

The mass of RIS was calculated by multiplying a sample's concentration of RIS by the total volume of formulation used for extraction from the area where the sample was collected. The concentration of RIS was determined by subtracting the spectra optical density (OD), of the formulation base from that of the samples', at the appropriate wavelength (280-nm or 315-nm, see above RIS formulation). Using this subtracted OD value and the wavelength's corresponding standard curve linear regression equation, the sample's RIS concentration was calculated (see Chapter 3).

Mass balance calculations were performed for all experiments to ensure a proper closed-system in the experimental set-up. The mass of RIS was quantified at the beginning and at end of the experiment. The initial mass of RIS was defined as the RIS dose (or RIS formulation) loaded into the delivery device which was determined from the analysis of a sample. The mass of RIS in the system at the end of an experiment was determined by sampling and quantifying the mass of RIS for parts of the experimental set-up (including the delivery device) that had contact with aerosol or formulation, and taking their sum to achieve the value for the total amount of RIS. The two total mass values of RIS were compared to ensure mass balance.

The stability of 5-mg/ml RIS in the prepared solution (25% PG; 25% EtOH: 50% H2O vol/vol/vol) was assessed and described previously in Chapter 2 (and Chapter 3). The same measure of stability will be applied within this Chapter.

Experiments were set-up as a closed system, and run in a ventilated hood with equipment that had been cleaned and dried: 70%-ethanol was sprayed and removed from equipment by evaporation or with Kim wipes, followed by being immersed under continuously flowing warm water, subsequently all equipment was soaked in de-ionized water for approximately 12-hours before being air dried for a minimum period of 12-hours to 24-hours. For e-cig experiments, the battery was charged and new cartridges/atomizers were used.

Prior to commencing each experiment, samples of the prepared RIS formulation and formulation alone were collected and UV/Vis spectra data was used to quantify its concentration and determine the mass of RIS contained in the initial dose. A precision scale was used to measure the mass of the delivery device the e-cig cartridge: empty and dry, loaded with the initial dose of RIS formulation, the end of the completed experiment. The voltage and resistance, of the e-cig's battery and atomizer respectively, were evaluated prior to their use.

An 8-stage Anderson Cascade Impactor (ACI) and 28.3-L/min suction pump was assembled according to the appropriate stage and plates. . The ACI and suction pump were connected with tightly fitted plastic tubing. The ACI was used with a 0.22-micrometer filter paper following the final collection stage to capture

RIS aerosol particulates/droplets with an aerodynamic diameter of $\leq$ 0.4-µm and to maintain a closed-system.

An adapter was created to connect the ACI to the E-cig (Figure 32). The adapter was formed from a distilled-water bottle cap, plastic tubing, silicon with added parafilm to close gaps, and a metal tube bit. The interior of the cap was molded to fit around, flush, and centered on, the ACI's inlet. A hole or opening, the approximate diameter of the plastic tubing, at the center of the cap was formed. One end of the plastic tube was (slightly) inserted into cap's opening and the connection was bonded and sealed with superglue. During experiments, the connection was additionally sealed with parafilm as a secondary measure. A second opening in the plastic tubing was created for the e-cig. A small section of metal tubing was inserted into the second end of the plastic tube; this was to maintain the suction pump's airflow through the adapter to the ACI.

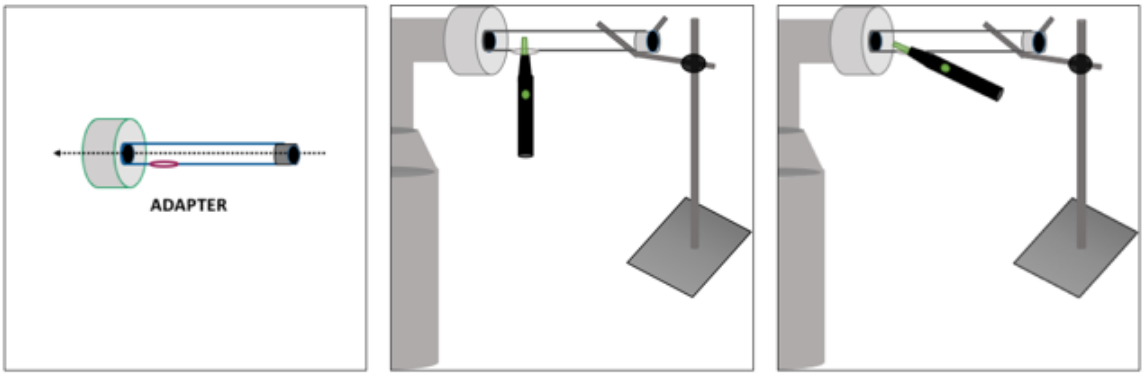

Figure 32 (from left to right) the adapter used for e-cig experiments to ensure ambient air flow was maintained during experimental run while supporting parallel and perpendicular placement of the emitted aerosol produced by the e-cig, experimental set-up of ACI and electronic cigarette while button is not depressed and while button is depressed and aerosol is emitted.

The adapter was placed around the opening of the ACI and sealed with parafilm to ensure a closed system. The opposite end of the adapter was supported by a lab stand hold the metal tubing to support and maintain an open atmospheric flow.

The relevant eGO-C® cartridge was weighed. Its mass was taken before being loaded with 1-ml of 5-mg/ml RIS solution. After being loaded with drug-solution, the cartridge's mass was taken again to confirm the mass measure of the initially loaded dose.

The atomizer was secured to the atomizer base, and the cover was screwed into place without overtightening. This step ensures proper airflow throughout the device, which is critical for aerosol production and emittance as well as the movement of the drug solution into the vapor production region of the device. The cartridge was inserted on to the atomizer, twisted slightly, and left to sit for 5-minutes to saturate the wick leading to the atomizer's coil for heating and

vaporization. Following this, the battery was connected and assembled. The connected e-cig device was vertically inserted into the opening of the plastic tubing, which was then sealed with parafilm. The set-up is shown in Figure 32.

The ACI was set-up as previously described. The suction pump was engaged for 5-minutes prior to the experiment and disengaged when the run was complete marked by the end of aerosol production.

The e-cig was engaged by manually depressing the button on the battery. During each depression, the e-cig was extended upwards (Figure 32) to simulate the behavior of cigarette smoking. The position of the e-cig during the vaporization was roughly horizontal, slightly negatively angled, with respect to the ACI's input.

The e-cig was engaged 3 times per minute. For each minute the e-cig was engaged 3-times, 10-seconds was the objective period of vaporization. This cycle ((3*10-seconds)/minute) was performed for a total duration of 15-minutes. The cartridge was tapped every few minutes and twisted around the atomizer by roughly 180 degrees every 5-minutes. The parafilm between the e-cig and plastic tubing was then checked to ensure its seal was maintained.

When the run was complete, the ACI was detached from the tubing connected to the suction pump. The ACI was disassembled and all parts (21 parts total) were separated into individual Ziploc-style closed plastic bags. The formulation was dispensed onto the bagged parts which were rubbed, wiped, shaken, and left to sit for 5 minutes. All items were treated as described in 'Sample and Data Collection'.

The adapter was placed into a Ziploc-style bag where the formulation vehicle was added. The filter paper was sectioned into halves or fourths before being placed in separate test tubes. The formulation was added and each test tube was centrifuged for 10 minutes at 13,500 rpm.

The e-cig was partially disassembled while keeping the atomizer section intact. The cartridge's mass was measured prior to being filled with the solution and re-inserted into the atomizer section. The cartridge and atomizer section were shaken and soaked together for 15-minutes. The resulting solution was collected into a test tube and the process was repeated until proper drug dissolution and concentration of experimental samples were achieved. The atomizer was disassembled from its set-up and taken apart before being placed in a test tube with added formulation base. The atomizer test tube was left to soak after being vortexed and shaken.

Samples were collected and observed as previously mentioned at 280-nm. Samples' OD at 280-nm were specifically observed during the sample collection and observation process to ensure it was within the respective standard curve range. If the OD extended past the standard curve's upper limit, more formulation (solution) base was added and the sample was re-taken. Sample concentration calculations included each sample extraction. This iterative process was performed (depending on the plate and amount of drug deposition) until the OD was appropriate for reading within the 280-nm absorbance-concentration detection range. The volume(s) of formulation added to extract deposited aerosolized RIS can be found in table Figure 33. Some values are based on

estimates, the exact values of added volume for drug dissolution was dependent upon the sample's OD reading during the collection and reading process, which

ACI Section	Volume of Formulation Base Added (ml)
Cartridge	~1.7
Atomizer	~17.0
Adapter w/ tube	0.6
Neck	~1.0
Throat	0.5
Filter Paper	~5.0
Stage Walls (0-7, F)	0.6
Plates 0 & 1	0.3
Plate 2	0.4
Plates 3 & 4	~0.6
Plate 5	~2
Plate 6	~2.7
Plate 7	~3
~Approximate Volumes Added	

Figure 33 General volumes added to individual ACI parts from the collection and assessment of RIS deposition

resulted in iterative dilutions (Figure 33).

Refer to Chapter 4 methods for the analysis and results of aerosol characterizing parameters and related values: mass balance, emitted dose, fine particle dose and fraction, aerodynamic particle diameter mass distribution, log ECD-cumulative distribution plot, regression analysis, MMAD and GSD.

5.3 RESULTS & DISCUSSION

Spectra profiles of RIS before (fresh preparations as control) and after ACI e-cig runs are shown for comparison in Figure 34, as a solid red line and dashed-black line respectively. Comparing RIS pre- and post- aerosolization, profile shape are generally consistent with each other. Aerosolized RIS spectra profile are absent of new peak formations suggesting degradation of aerosolized emitted RIS did not occur given no new chemical compounds were formed. Thus, delivered RIS was concluded to be stable which suggests the drugs safety. The safety and pharmacological integrity of RIS were technically confirmed as feasible based on the assessment UV/Vis collected data and measures.

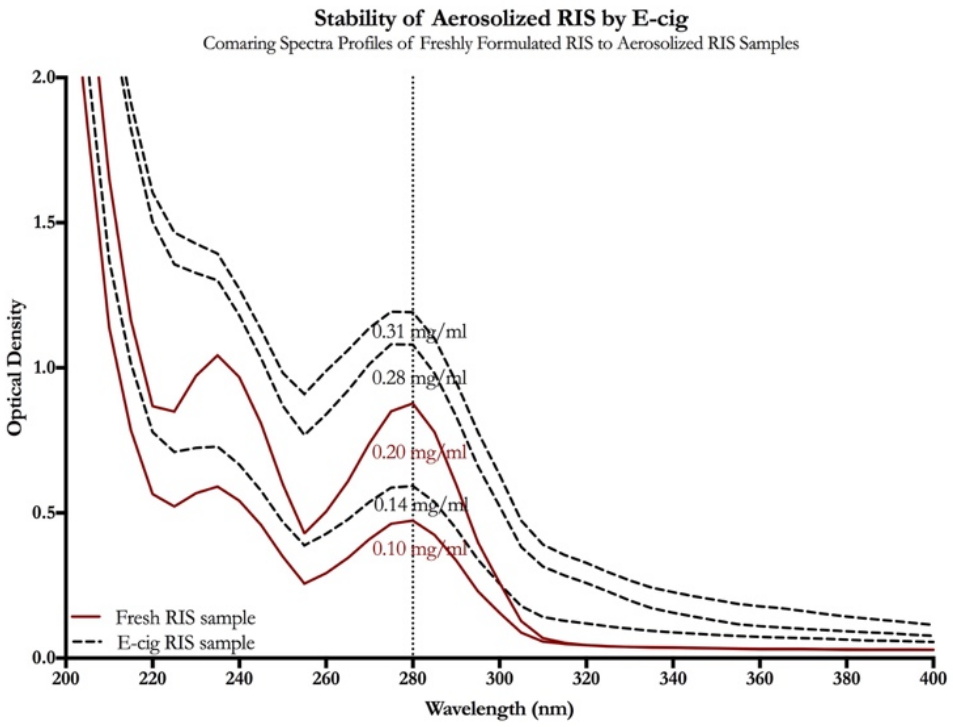

Figure 34 comparing spectra profile shapes of RIS for evaluating stability of drug aerosolized by an electronic cigarette against control samples of freshly prepared solution samples

Plates were observed to have drug particle deposition that was uniform in both deposition pattern and round droplet shape after run collection. The filter paper and stage plate F was observed to have particle deposition of yellowish color. The coloration could be the result of some thermally derived drug degradation or burning components within the e-cig itself given it's an unregulated device. Inter-stage losses to the ACI walls accounted for less than 1% of RIS mass found within the ACI.

ACI collected spectra profiles do not show definitively observable deviations between aerosolized and freshly prepared RIS, specifically the lack a new peak formation given what might be considered observable signs of drug degradation might be of concern. However slight deviations are seen. The 240-nm peak absorbance wavelength is less pronounced, and the profiles after 300-nm of aerosolized RIS increase in OD compared to the fresh preparation examples. These results provide evidence that suggests alternate measures to UV/Vis should be employed for further assessment.

Experimental integrity was confirmed by way of mass balance and drug recovery, as well as result reproducibility. Mass balance was assessed and compared across the entire system before and after experiment runs. The total mass recovery of RIS was at found to be greater than 95% of the initial dose. ACI results of runs 1 & 2, are shown in Figure 36 and Figure 35. Runs 1 & 2 were qualitatively observed as comparable and qualitative results were consistent between the two independent experimental runs (1 & 2). Consistent results between the experimental runs supported to general integrity of methodology given e-cigs are unregulated and achieving similar products within the same brand and product is a challenge. Therefore, experimental methodology was validated: experimental set-up, sample collection, quantification, assessment and analysis of data. Subsequently, results were considered representative of drug loaded aerosol that would be delivered to patients.

The total mass of RIS captured within the ACI (sum of RIS on all components: the adapter, all stage walls and plates from 0 - F, filter paper) for run 1 was 2.8-mg or 48.2% of the initial dose of RIS mass, and the same measures for run 2 was 3.5-mg or 61.6%. The emitted dose of RIS, the sum of RIS mass on all plates (0-7, F) reported as the percent fraction of the total ACI RIS mass, was 47.9% and 61.6% (run 1, 2).

The aerodynamic particle diameter distribution (APDD) is shown in Figure 36. The APDD shows the mass of RIS on each stage plate (0-7, F) as a percent fraction of the total emitted dose plotted against the associated aerodynamic particle diameter (APD) stage band range. The dot-line plotted on the APDD shows the average of both runs (dot) and distribution shape. The fine particle fraction (FPF) and fine particle dose (FPD) is defined in the previous literature as the mass sum of drug < 5 micrometers (aerodynamic particle diameter range).

FPF and FPD were calculated as the mass of RIS summed over stage plates 3-F (<4.7 micrometers, stage plates 3, 4, 5, 6, 7, F) and the FPF was calculated as the percent fraction of the FPD over the total emitted RIS dose. The FPF was calculate to be 60.9% and 58.0% (run 1, 2) of the total emitted dose of RIS mass found on all plates. The FPD (fine particle dose) of RIS mass particles $\leq$4.7 micrometers in aerodynamic diameter was found to be: 2.7-µm and 3.5-µm (run 1, 2).

The cumulative distribution of RIS mass on each stage plate below the effective cut-off aerodynamic diameter (ECD) of the previous stage is shown in Figure 36 as a percent fraction of the total emitted RIS dose. Runs 1 & 2 were graphed together and regression analysis was performed for all plotted data points in Figure 35. A combined linear model best fit the plotted data points. The resulting best-fit line equation was calculated and shown in Equation 6 and an R^2 of 0.99.

$$y = 0.40x - 20.5$$

Equation 6 line equation resulting from the regression analysis of the log((ECD)-prohbit scale cumulative distribution plot of runs 1 & 2 combined.

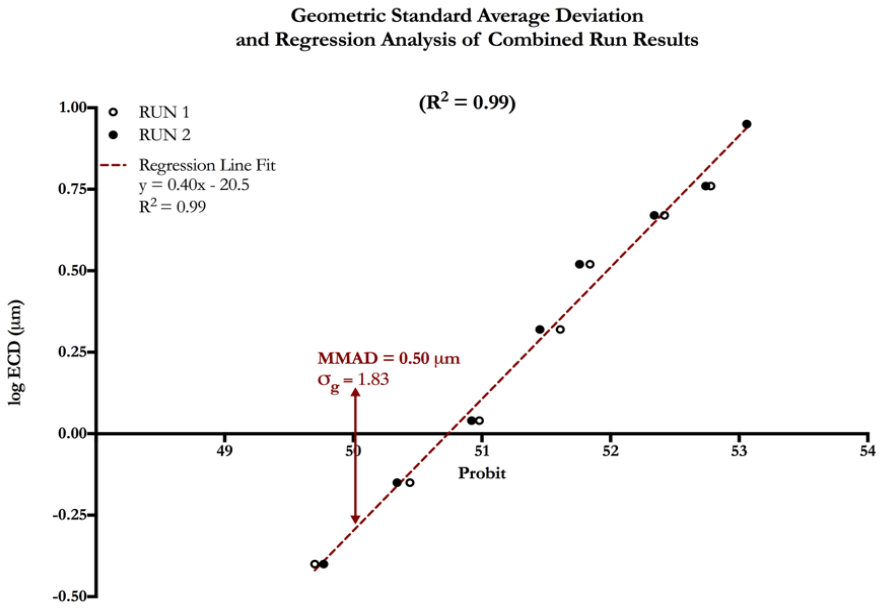

Figure 35 Regression Analysis and resulting MMAD and GSD calculations. Graph of log ECD and cumulative distribution on prohbit scale plot

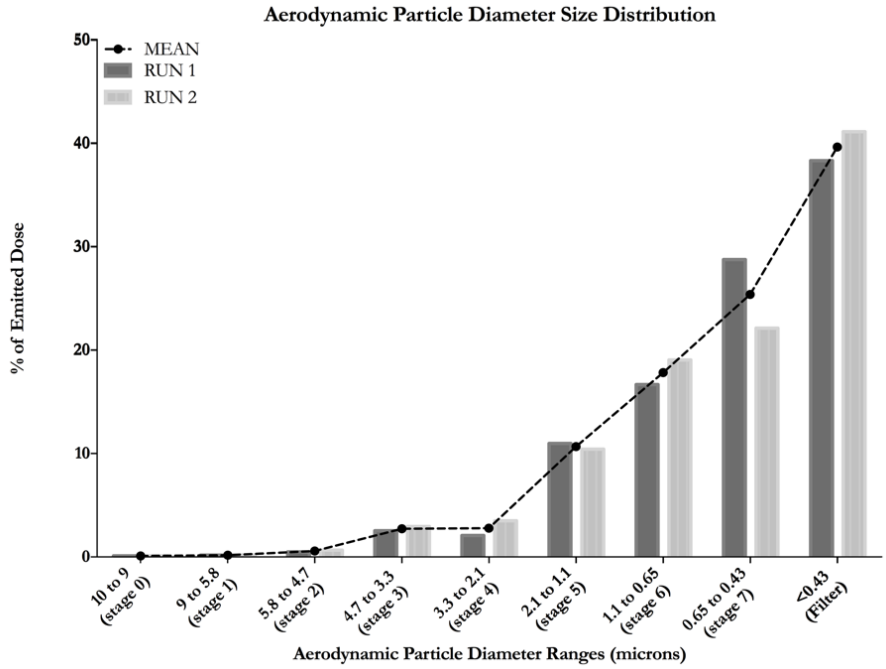

Figure 36 The aerodynamic particle diameter distribution of RIS as a percent fraction of the emitted dose

The line equation (Equation 6) was used to determine the mass median aerodynamic diameter (MMAD) and the geometric standard deviation (GSD). The MMAD was defined as the aerodynamic particle diameter of RIS associated with the cumulative distribution of RIS mass at 50%, The resulting MMAD of RIS was found to be 0.50 micrometers.

A secondary value of MMAD was calculated by performing another regression analysis and re-calculating the result for the same data not including mass RIS found for F. The line equation had an R^2 of 0.98 and the MMAD value was found to be 0.79 micrometers. The aerodynamic particle diameter (APD) range associated with systemic drug uptake within the deep lung is $\leq 2 - 3$ micrometers. However very small APD measures are likely to be exhaled as opposed to deposit in the desired pulmonary region (48). The MMAD nonetheless is within the desired < 2-3 micrometer range and supports the feasibility of delivering aerosolized RIS to the deep lung using an e-cig as a delivery device. The GSD or the cumulative mass distribution of RIS aerodynamic particle diameter spread with respect to the MMAD, was found to be 1.83. The GSD value suggest particles vary in aerodynamic diameters around the MMAD, seen in Figure 36 and Figure 35. Compared to the jet nebulizer APDD results in Figure 28, RIS aerosolized and emitted from the e-cig has an APD of predominantly <2.1 micrometers (stage 5 or below).

The total sum of RIS mass in the APD ranges between 0.43 - 2.1 micrometers. This range is associated with the pulmonary region associated with systemic uptake. The available delivered deep lung dose was an averaged to be 1.7-um (+/- 0.2-um). The deep lung dose exceeds the optimal delivered dose of 1-mg required to achieve a therapeutically relevant exposure-effect drug profile to address schizophrenia related symptoms. The initial assessment of technical feasibility relating to the systemic delivery of a therapeutic RIS dose for the treatment of schizophrenia by inhaled administration and pulmonary delivery was determined to be valid based on a preliminary assessment from the results described above here within.

6. ASSESSING **TECHNICAL FEASIBILTY**

In Table 7 feasibility criteria in relation to results were defined. In Table 7, the criteria defining the technical feasibility requirements were defined and result were summarized in the column titled 'technical assessment' based on the contained experimental findings within this document. The document chapter containing the relevant results and findings that address the feasibility criteria

FEASIBILITY			
CRITERIA	DESCRIPTION	TECHNICAL ASSESSMENT	DETERMINED AND EXPLORED IN:
SAFETY	Drug remains stable in solution	YES	CH 3
	Drug prepared in solution use excipients that are FDA approved as safe for the given application	YES	CH 3
	Realistic storage conditions for drug stability	YES	CH 3
	Drug is stable after being aerosolized	YES	CH 4 (&5)
EXPERIMENTAL DEVELOPMENT	Mass balance is within +/-15% of initial dose experimentation	YES	CH 4 (&5)
	The solution – aerosol delivery device combination is functional with selected representative devices specifically a jet nebulizer	YES	CH 4
	ACI methodology is developed such that results are reproducible (mass balance is maintained)	YES	CH 4 (&5)
AEROSOL CHARACTERISTICS ARE APPROPRIATE FOR THE DESIRED DELIVERED DOSE OUTCOME WHILE BEING PRACTICAL	The concentration of drug in solution is maximized to theoretically achieved the optimal delivered dose	YES	CH 3
	The delivered dose is achieved without surpassing the device's volume limitations	YES	CH 4 (&5)
	The delivered dose is achieved within an administration time frame that is reasonable (<20 minutes, determined based on other nebulized administered drug time frames).	YES	CH 4 (&5)

Table 7 Review of Feasibility Criteria Overview and technical feasibility Evaluation

explored for determining the 'technical assessment' outcomes are listed in the column on the most right-side of Table 7.

Chapter 3 provided a pre-formulation assessment of Risperidone in a solution comprised of the following excipients: propylene glycol (25%), 95% (vol/vol) ethanol (25%) and H_2O (50%) (vol/vol/vol). The selected excipient and their respective amounts were approved by the FDA as safe for use in a solution to be aerosolized and administered to the pulmonary route. The concentration of a 5-mg/ml Risperidone solution was confirmed and stress temperature-time tests were performed for further assessment of the prepared drug-solution.

Vials containing 5-mg/ml RIS solution were stored in triplicates at temperatures of: 4°C, 24°C, and 37°C. Samples were collected over a duration of 96-days. Results concluded that 5-mg/ml RIS solution stored at 24°C was maintained a drug-concentration over time within reasonable proximity to that of the initially prepared solution. Additionally, no new peak formations were observed within the spectral profiles of samples collected. The RIS prepared solution did not degrade when stored at room temperature over the time of assessment. Samples from the solution base prepared without drug, shows signs of instability and/or contamination.

The 5 –mg/ml Risperidone solution was comprised of approved FDA excipients for this application while achieving a theoretically feasible concentration of Risperidone in solution to support further experimentation of feasibility with respect to technically delivering a therapeutically-relevant deep lung dose of Risperidone of the treatment of Schizophrenia. Collected spectra profiles of varied Risperidone solution concentrations (fresh preparations) in Chapter 3 as a control, aerosolized Risperidone by both Jet nebulizer and electronic-cigarette were compared for stability. Spectra profile comparisons indicate that Risperidone remains stable when delivered by aerosol administration. Risperidone aerosolized by an electronic cigarette does not indicate the formation of any degradation products however signs of potential impact due to thermal energy on the drug's integrity is an item for consideration.

The 5-mg/ml Risperidone solution could function with both the jet nebulizer and the electronic cigarette to produce and emit drug-loaded aerosol. This further validates the solution preparation of Risperidone used in the above.

6.1 ASSESSING TECHNICAL FEASIBILTY: JET NEBULIZER & ELECTRONIC CIGARETTE

The experimental methodology was carefully designed and meticulously assessed to ensure the integrity of: set-up, collection, quantitation/measures, results, and aerosol analysis. To summarize methodology (see Chapter 4 & 5 for more in depth description) validation, the mass drug recovery for all reported experiments were within 95% of the initial starting drug mass (or +/- 5% mg). The experimental methodology required to achieve sound results for analytical purposes from an 8-stage Anderson Cascade Impactor and under the given conditions requires precision and accuracy. The results and analysis described above, indicate high experimental integrity despite the limited consecutive experiment iterations reported.

The jet nebulizer and the electronic cigarette were selected as representative systems to evaluate the technical feasibility of delivering a therapeutically relevant deep lung dose of Risperidone for the treatment of schizophrenia related symptoms. Both representative devices successfully delivered a deep lung dose of Risperidone (mass sum of aerosolized Risperidone ADPD size ranging between 0.4-micrometers - 3.0-micrometers) greater than the optimal 1-mg deep lung dose found in Chapter 2. At 5-mg/ml Risperidone in solution the volume required to deliver the therapeutic deep lung dose did not exceed the devices' maximum volume capacity. The duration of administration was required to be $\leq$20-minutes for both devices (the administration time threshold that was determined). The 20-minute administration time capacity was

determined based on administration times that have been previously viewed in association with a jet nebulizer. Tidal breathing, the ratio of inhalation and exhalation was 50:50 under the assumption of normal pulmonary function.

Given the above and using aerosol characterizing parameters (jet nebulizer and electronic cigarette), deep lung ADPD size range and drug concentration, the volume and time of aerosolization required to achieve a delivered 1-mg dose of RIS to the deep lung was determined and evaluated.

The jet nebulizer was continuously run over time. The delivered 1-mg dose were based on the determined 0.35 ml-min volumetric flow rate of emitted aerosol by jet nebulization. The jet nebulizer was assumed to have a dead volume requirement of 1-ml. Thus, the total initial volume required to achieve the 1-mg delivered dose included the addition of 1-ml RIS solution. The time required to deliver a 1-mg dose by continuous jet nebulization was doubled to account for the inhalation: exhalation reparatory cycle ratio.

Thus, the jet nebulizer loaded with 5.0-mg/ml RIS solution was found to deliver a 1-mg deep lung delivered dose in approximately 2.5-minutes (2.44-minutes) from an initially loaded volume of 1.86-ml of solution.

An electronic-cigarette will deliver 1-mg of Risperidone to the deep lung after approximately 9-minutes (8.64-minutes) of time. The time-frame is based on the following administration criteria: 30-seconds of administration (respiration)

time and 30-seconds of exhalation for each 1-minute duration, intervals of inspiration/exhalation are each 10-second. A 0.53-ml volume of 5-mg/ml RIS solution was required to achieve a 1-mg delivered dose. However, the values assume that a 1-ml volume of 5-mg/ml Risperidone solution was loaded into the electronic-cigarette container. The 1-ml volume was used as constant solution saturation of the wicking material is required for proper aerosolization of drug solution. Otherwise the wick material will be burned by the coil and likely increased risk thermal drug degradation. Due to the decreased volume capacity of the electronic cigarette as compared to the jet nebulizer cup, the determination of required dead volume for proper wick material saturation was not adequately determined.

An initial pre-clinical technical assessment of using the pulmonary route for drug delivery was performed using the FDA-approved Anderson Cascade Impactor. Based on the resulting analysis for two representative delivery device systems (jet nebulizer, electronic-cigarette), the delivery of a deep lung therapeutically-relevant dose of 1-mg Risperidone for the treatment of schizophrenia related symptom was concluded as feasible.

7. OVERALL DISCUSSION

Various elements of these experiments could be expanded and possibly improved. A discussion of how to capitalize on this work and improve future efforts follows.

A 5-mg/ml Risperidone solution was prepared using FDA approved, safe excipients (GRAS). The FDA approved the following excipients as safe for a solution delivering a pharmaceutical agent by pulmonary administration as safe: 25% vol/vol ethanol (95%), 25% vol/vol propylene glycol. The remaining 50% volume of the prepared solution was water (H_2O). Experiments should be performed with the inclusion of a secondary assay (methodology) to UV/Vis for the detection, quantification and assessment of Risperidone (i.e. HPLC or other detection methods used in previous literature cited in Chapter 3).

The 5-mg/ml Risperidone solution requires further investigation. The observed new peak formation (degradation) found in samples collected from vials of the solution base (0-mg/ml-RIS solution) stored over time (4ºC, 25 ºC, 37ºC) indicates the need for further testing and/or development of the solution preparation used here within. Additionally, longer-term observation and assessment of a RIS solution is needed to prove adequate drug stability for clinically-applied purposes (stability for one-year minimum).

A standard jet nebulizer (PARI LC® ® ®) was used as a representative delivery device system along with the prepared 5-mg/ml RIS solution for characterizing emitted aerosol, which was performed with an 8-stage Anderson Cascade Impactor. The results were quantified using UV/Vis and subsequently analyzed for feasibility delivering a stable, therapeutically-relevant delivered dose for schizophrenia treatment to the deep lung region (systemic uptake). The jet nebulizer is a well-researched, inexpensive delivery device. The PARI LC® ® ® jet nebulizer is FDA approved and regulated as a delivery device for therapeutically delivering aerosolized drug prepared in a compatible solution formula. Technical feasibility was centered around the analysis of the aerosol characterization generated by the jet nebulizer delivery device and the 5-mg/ml RIS solution. The aerosol characterization analysis confirmed that the desired pulmonary delivery objective was technically feasible.

Given technical feasibility was confirmed using a jet nebulizer as the delivery device an electronic-cigarette was assessed using the same technical feasibility criteria. Unlike the jet nebulizer, an electronic-cigarette is not approved by the FDA for the therapeutic delivery of pharmaceutical agents. Moreover, the electronic-cigarette is a device that is completely unregulated. To the best of my knowledge, the electronic-cigarette has not been assessed as a platform for the delivery of prescription pharmaceuticals (nicotine; or marijuana which is an alternative drug therapy), such as psychotropic agents, for therapeutic treatment

purposes. The electronic-cigarette is a device that is accessible and inexpensive, while being simple to customize or manipulate.

The electronic cigarette devices are unregulated, such that items are variable (products may be inconsistent), and quality control is virtually nonexistent. This was found to be particularly true with respect to the atomizer (wick and coil) component of the electronic cigarette device. The atomizer product inconsistencies were found despite purchasing the same brand & model of atomizer from the same online website. There was significant variability between brand blister atomizer packs (3 atomizers per pack, 3-atomizers in blister pack were consistent). Experiment results were consistent but only when using atomizers from the same blister pack and only when each atomizer was used for one experimental run. In addition, the container holding volume of solution was carefully selected and volume capacity was measured to ensure consistency due to occasional variability.

These result variations occurred despite checking for and ensuring consistent atomizer resistance and battery voltage. The wick contained within the atomizer is likely a contributing factor to inconsistencies. The wick may be formed of different materials, coated, or saturated with primer before being packaged for use. The atomizer coil construction and material is likely another contributing factor.

However, component reliability and consistency can be achieved by electing to independently construct the atomizer (wick included) and/or modify

device components to improve result reproducibility. The electronic cigarette components are easily accessible for modification, as well as simple in construction and function. Online communities and forums, including video examples, are readily available for atomizer modifications or different wick/coil set-up constructions. A plethora of atomizers are designed for the sole purpose of allowing the user to independently construct their desired atomizer set-up. Thus, modifying the device atomizer component to better control experimental reproducibility is possible and should be further explored.

Assuming a stable 5-mg/ml RIS solution, further jet nebulizer experiments using the ACI should be performed with the objective of experimentally achieving a 1-mg delivered dose in the region associated with systemic uptake. These ACI experiments should be performed with an attached ventilator or respiratory simulation device for assessment purposes. Experiments should be calibrated based on the objective of delivering almost exactly 1-mg of RIS to the deep lung. Experimental set-up should be extensively repeated to maximize experimental specificity and sensitivity of delivering the 1-mg dose. The results should be statistically analyzed to evaluate the corresponding variability of delivering a 1-mg dose by pulmonary administration. The error margin of the delivered dose should be evaluated at upper and lower limits to determine the likelihood of potential risks.

For a 1-mg delivered dose, the corresponding amount of aerosolized drug likely to be orally ingested should be calculated. The ingested dose should be evaluated to determine its impact on the drug's exposure – effect profile. Depending on the outcome, the PK-PD model based simulations and the optimal dosing regimen should be re-evaluated.

Characteristics of the jet nebulizer given the RIS solution should be more thoroughly explored and defined. Jet nebulizer experiments should be performed and repeated for reproducibility, under thoughtfully varied planned conditions to improve robustness (reduced concentration of RIS, respiratory cycles above and below assumed normal inhalation: exhalation, 50%:50%, alternate delivered dose (not 1-mg), different jet nebulizers and/or inter-device variations).

The ACI experiments utilizing the electronic cigarette as a delivery device had limitations that are addressable in the future should further experimentation be pursued. Limitations that were most notable are as follows: purchased atomizers of the same brand and type varied with results being reproducible for atomizers within the same 4 atomizer blister pack. Human error was difficult to avoid and to account for given the device required a button to be depressed to produce aerosol with the main consistency factor being the devices' 15–sec safety shut-off.

Future assessments of drug delivery using an electronic cigarette should independently construct the interior of the atomizer element (wick and coil). The atomizer should be adjusted and constructed, utilizing selected fiber and coil material to achieve experimental reproducibility and result consistency that is not dependent upon the purchase of unpredictable products developed without product quality control while considering or improving its compatibility with RIS.

The battery shut-off should be experimentally adjusted and controlled to reduce human error. The shut-off time frame should be determined based on initial preliminary testing to determine the experimental methodology. A device that modulates the temperature of the emitted aerosolized vapor production would be an improvement.

The thermal degradation of Risperidone should be further assessed within the context of aerosol production and temperatures from the electronic cigarette. Implementing the above adjustments to the experimental methodology and set-up should provide results that are not impacted by potentially significant product variability.

7.1 ADDRESSING ADHERENCE

The customizability of the electronic cigarette along with being powered provides an unusual opportunity for monitoring consumer's adherence to pharmacological treatment, specifically the treatment population (schizophrenia) addressed within this document for improving patients' therapeutic treatment

adherence. Adherence to therapeutic treatments is low within the population being addressed. The lack of adherence presents treatment issues such as an increasing prescribed drug dosage based on the assumption of adherence and lack of medication efficacy.

Moreover, there are limited ways of monitoring a patient's treatment adherence in an outpatient setting. Studies indicate that providers overestimate patients' adherence, and patient' adherence is lower than is actually reported. Adherence monitoring is limited typically to a pill-bottle cap counter that records the number of time the bottle cap is opened. This system of adherence monitoring is easily tampered with. Adherence can be more reliably monitored utilizing a pulmonary delivery device platform like that of an electronic cigarette as it would be harder to tamper with.

Alternately studies evaluating therapeutic impact or related factors within an outpatient population might be more easily able to monitor and accurately report results if adherence or administered drug amount could be accurately reported. The electronic cigarette might offer an experimental platform for the design of delivery devices. The rapid uptake of inhaled systemically delivered drug dosages might be an opportunity for anti-anxiety, sleep, or pain medication with rapid impact and high abuse potential to be exchanged for less habit and dependency forming substances with the ability to rapidly impact the distressing symptom. Monitoring patient's adherence (over or under) to dependency forming

or addictive drugs can be useful in various circumstances benefiting the provider and/or the patient. Other applications might be general pain relievers, anti-nausea (even within hospital settings to avoid injection), or anti-anxiety medications inhaled for distress, agitation, or for patients with phobias such as to needles when getting blood drawn. Improved reliability in adherence monitoring could provide useful for both providers and their patients with low executive functioning (ex. low memory) such the aging or geriatric population.

8. FUTURE: IMPLICATIONS & DIRECTIONS

The prepared 5-mg/ml Risperidone solution requires further investigation. The new peak formation (degradation) found in samples collected from vials of the solution base (0-mg/ml RIS) stored over time (at temperatures of 4C, 25C, 37C) indicates the need for further testing and or development of the solution preparation used here within. Additionally, longer-term observation and assessment of a RIS solution is needed to prove adequate drug stability for clinical purposes (at least one-year showing stable results).

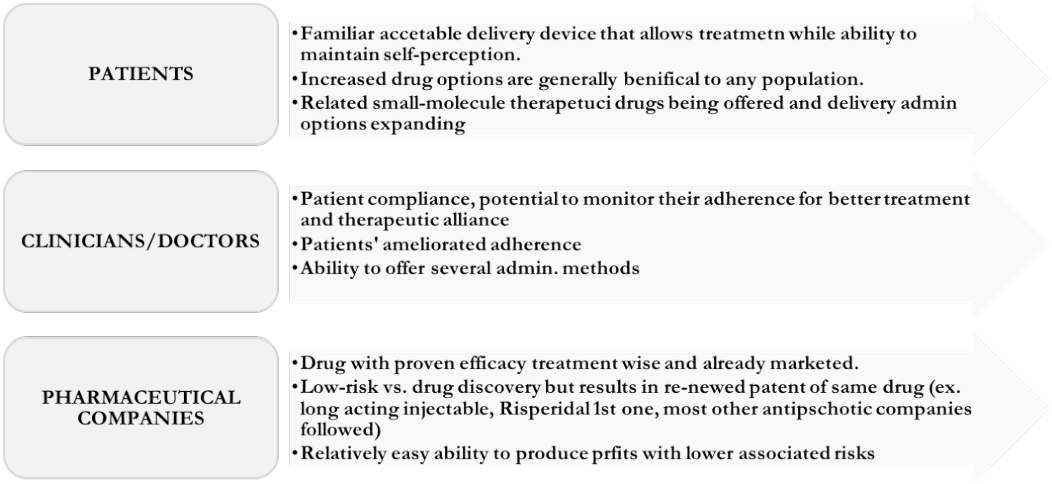

Figure 38 Stakeholders immediately relevant in assessment of cost-benefit analysis

The antipsychotic dose for the treatment of schizophrenia related symptomology is greater than the antipsychotic dosages for any alternate

pharmacological treatment application purposes. RIS, administered to the pulmonary route for the therapeutic treatment of schizophrenia, was found to be technically feasible based on the optimal dosing regimen determined for the extensive metabolic phenotype (80% of population). Extensive metabolizers are more likely to require a higher dose to achieve therapeutic effect than poor metabolizers. RIS for the treatment of alternate illnesses and/or different metabolic phenotype(s) administered to the pulmonary route will be able to achieve a lower delivered dose required for achieving relevant therapeutic exposure-effect. Subsequently, technical feasibility can be inferred based on the evaluation criteria previously defined here within.

Technical feasibility of the pulmonary delivery route for drug administration was assessed based on the following representative delivery devices: the jet nebulizer and electronic cigarette. The jet nebulizer was the only representative drug delivery device system for technical assessment of feasibility that was approved for pharmaceutical-drug therapy by the FDA. The electronic cigarette is an unapproved and unregulated delivery device that used a secondary delivery device that provided user-behavior approximated smoking of a standard cigarette. Technical feasibility requires the assessment of an array of representative delivery device systems. For a review of technical feasibility, representative aerosol delivery device(s) should be selected and assessed based on your target product profile. Target product profile should be further explored for robustness.

Technical feasibility was assessed for the preliminary preclinical data evaluation for estimating the likelihood of achieving successful results for treatment of the target population by pulmonary drug delivery. Results of the technical feasibility assessment was intended to be used as evidence in support, or against, exploring the pulmonary route for delivering the treatment-relevant dose of drug (RIS). The value of a thorough technical feasibility assessment review utilizing an array of devices is not of utility should there be no externally-defined reason for further progressing the above experiments to a clinical testing phase.

A cost-benefit analysis should be defined for the evaluation of resources, defining the project limits for discontinuation. Future study implications should be based upon stakeholders' interest and investment, and incorporated within the cost-benefit analysis. Future development and exploration of the above should be pursued only if there is reason (stakeholder mentioned or otherwise, see Figure 38) to concretely determine whether advancing towards clinical trial, testing schizophrenia symptoms treatment by the pulmonary delivery of RIS.

Electronic-cigarettes are operated utilizing battery power. Battery operated devices, including those in existence, allow users to control the wattage/voltage and temperature, which are based upon the atomizer's construction determining the resistance of atomizer and the coil and wick material, as well as the airflow directed throughout the device by atmospheric air intake near the atomizer element varied by diameter and number of region for air intake (produced

temperature/pressure differential, draws liquid solution through the wick to vapor coil region, general electronic cigarette functional parameter impacting aerosol production and should be controlled for results reproducibility).

Even the most basic electronic cigarette devices can track the number and duration (individually) of inhaled respiratory administration. Based on the device's battery-based power, microchips can be programmed and added to the battery power device. Alternatively, a programmed battery device is likely easily modifiable by manipulating the already existing elements. The unregulated nature of the electronic-cigarette can offer advantages that regulated devices cannot.

The electronic-cigarette could provide a unique platform for several applications. The electronic-cigarette has experimental applications and utility as a low-cost, easily modifiable aerosol drug delivery platform. There is no risk to expensive equipment and no oversight is required given a nonexistent learning curve. **This could provide a unique approach to monitoring and addressing patients' pharmacological treatment adherence.**

The electronic-cigarette as a drug delivery platform should be thoroughly characterized to evaluate its utility and functionality. Experiments should be set-up to evaluate aerosol production based on varied device and solution parameter combinations. Device Parameters should be independently assessed and

iteratively adjusted. The electronic cigarette device should be assessed for changes in vapor production based on changes in: atomizer (resistance, set-up design, wick and coil material), airflow intake surrounding the atomizer (diameter and number of inlet holes). Solution related descriptors should be evaluated for changes in vapor production from the combined impact of solution parameters given other factor(s): viscosity, drug-concentration, density, loaded solution volume, excipient factor of influence (i.e, rate of evaporation). Produced and emitted aerosol changes based on the impact of user administration behavior: suction, inhalation time and related volumetric flow rate, other factors such as angle of device.

9. CONCLUSION

These experiments demonstrate the feasibility of administering clinically-relevant therapeutics in a manner that may improve adherence for traditionally problematic patient populations. Clinicians, patient advocates, patients, and others have a vested interest in improving the treatment of patients that have thus far been difficult to treat in the real world. The experiments described here present a novel method to administer medications such that the process of treatment doesn't "feel" like taking pharmaceuticals. This approach offers several novel marketing approaches and patient-adherence strategies to a clinical setting that has seen very little innovation in the past 20 years.

Although there is certainly rigorous science to be done in exploring e-cigarette based delivery of anti-psychotics, these experiments demonstrate real-world feasibility. The next big question is how do we translate these results into preliminary clinical studies. The drugs and excipients are safe, and the means to deliver them is readily available and easily implemented.

10. REFERENCES

1. Tomar RS, Joseph TJ, Murthy AS, Yadav DV, Subbaiah G, Krishna Reddy KV. Identification and characterization of major degradation products of risperidone in bulk drug and pharmaceutical dosage forms. J Pharm Biomed Anal. 2004;36(1):231-5.

2. Bharathi C, Chary DK, Kumar MS, Shankar R, Handa VK, Dandala R, et al. Identification, isolation and characterization of potential degradation product in risperidone tablets. J Pharm Biomed Anal. 2008;46(1):165-9.

3. Wu EQ, Birnbaum HG, Shi L, Ball DE, Kessler RC, Moulis M, et al. The economic burden of schizophrenia in the United States in 2002. J Clin Psychiatry. 2005;66(9):1122-9.

4. Tandon R, Nasrallah HA, Keshavan MS. Schizophrenia, "just the facts" 4. Clinical features and conceptualization. Schizophr Res. 2009;110(1-3):1-23.

5. Carpenter WT, Koenig JI. The evolution of drug development in schizophrenia: past issues and future opportunities. Neuropsychopharmacology. 2008;33(9):2061-79.

6. Batel P. Addiction and schizophrenia. European Psychiatry. 2000;15(2):115-22.

7. Crump C, Crump C, Winkleby MA, Winkleby MA, Sundquist K, Sundquist K, et al. Comorbidities and mortality in persons with schizophrenia: a Swedish national cohort study. American Journal of Psychiatry. 2013;170(3):324-33.

8. Villalta-Gil V, Vilaplana M, Ochoa S, Haro JM, Dolz M, Usall J, et al. Neurocognitive performance and negative symptoms: Are they equal in explaining disability in schizophrenia outpatients? Schizophrenia research. 2006;87(1-3):246-53.

9. Liu KC, Chan RC, Chan KK, Tang JY, Chiu CP, Lam MM, et al. Executive function in first-episode schizophrenia: a three-year longitudinal study of an ecologically valid test. Schizophr Res. 2011;126(1-3):87-92.

10. Breier A, Schreiber JL, Dyer J. National Institute of Mental Health longitudinal study of chronic schizophrenia: prognosis and predictors of outcome: Archives of …; 1991. 239-46 p.

11. BROWN S, Barraclough B, INSKIP H. Causes of the excess mortality of schizophrenia. The British journal of psychiatry. 2000;177(3):212-7.

12. Capasso RM, Capasso RM, Lineberry TW, Lineberry TW, Bostwick JM, Bostwick JM, et al. Mortality in schizophrenia and schizoaffective disorder: an

Olmsted County, Minnesota cohort: 1950–2005. Schizophrenia research. 2008;98(1-3):287-94.

13. <1999 Tandon.pdf>.

14. Huber G, Gross G, Schüttler R, Linz M. Longitudinal studies of schizophrenic patients. Schizophrenia Bulletin. 1980;6(4):592-605.

15. Albus M. Clinical courses of schizophrenia. Pharmacopsychiatry. 2012;45 Suppl 1:S31-5.

16. Schmael C, Georgi A, Krumm B, Buerger C, Deschner M, Nothen MM, et al. Premorbid adjustment in schizophrenia--an important aspect of phenotype definition. Schizophr Res. 2007;92(1-3):50-62.

17. Klosterkötter J, Klosterkötter J, Schultze-Lutter F, Schultze-Lutter F, Ruhrmann S. Kraepelin and psychotic prodromal conditions. European archives of …. 2008.

18. Hiroeh U, Appleby L, Mortensen PB, Dunn G. Death by homicide, suicide, and other unnatural causes in people with mental illness: a population-based study. The Lancet. 2001;358(9299):2110-2.

19. Janssen PA, Niemegeers CJ, Awouters F, Schellekens KH, Megens AA, Meert TF. Pharmacology of risperidone (R 64 766), a new antipsychotic with serotonin-S2 and dopamine-D2 antagonistic properties. Journal of Pharmacology and Experimental Therapeutics. 2006;244(2):685-93.

20. Leucht S, Barnes T, Kissling W. Relapse prevention in schizophrenia with new-generation antipsychotics: a systematic review and exploratory meta-analysis of randomized, controlled trials. American Journal of Psychiatry. 2003;160(7):1209-22.

21. Feng Y, Pollock BG, Coley K, Marder S, Miller D, Kirshner M, et al. Population pharmacokinetic analysis for risperidone using highly sparse sampling measurements from the CATIE study. Br J Clin Pharmacol. 2008;66(5):629-39.

22. Patton JS, Byron PR. Inhaling medicines: delivering drugs to the body through the lungs. Nat Rev Drug Discov. 2007;6(1):67-74.

23. Nasrallah HA, Targum SD, Tandon R, McCombs JS, Ross R. Defining and measuring clinical effectiveness in the treatment of schizophrenia. Psychiatr Serv. 2005;56(3):273-82.

24. West JC, Marcus SC, Wilk J, Countis LM, Regier DA, Olfson M. Use of depot antipsychotic medications for medication nonadherence in schizophrenia. Schizophrenia bulletin. 2007;34(5):995-1001.

25. Gary JR, Martha EA. Depot neuroleptic therapy: clinical considerations. The Canadian Journal of Psychiatry. 1995;40(3_suppl):5-11.

26. Palmer BW, Dawes SE, Heaton RK. What Do We Know About Neuropsychological Aspects Of Schizophrenia? Neuropsychology Review. 2009;19(3):365-84.

27. Bhanji NH, Chouinard G, Margolese HC. A review of compliance, depot intramuscular antipsychotics and the new long-acting injectable atypical antipsychotic risperidone in schizophrenia. Eur Neuropsychopharmacol. 2004;14(2):87-92.

28. Byron PR. Drug delivery devices: issues in drug development. Proc Am Thorac Soc. 2004;1(4):321-8.

29. Noymer PD, Myers DJ, Cassella JV, Timmons R. Assessing the temperature of thermally generated inhalation aerosols. J Aerosol Med Pulm Drug Deliv. 2011;24(1):11-5.

30. <2009 FDA.pdf>.

31. Cramer JAJ, Cramer JA, Rosenheck R, Rosenheck RR. Compliance With Medication Regimens for Mental and Physical Disorders. Psychiatric Services. 1998;49(2):196-201.

32. Lindström E, Bingefors K. Patient compliance with drug therapy in schizophrenia. Pharmacoeconomics. 2000;18(2):105-24.

33. Byerly MJ, Nakonezny PA, Lescouflair E. Antipsychotic medication adherence in schizophrenia. Psychiatric Clinics. 2007;30(3):437-52.

34. Byerly MJ, Thompson A, Carmody T, Bugno R, Erwin T, Kashner M, et al. Validity of electronically monitored medication adherence and conventional adherence measures in schizophrenia. Psychiatr Serv. 2007;58(6):844-7.

35. Hudson TJ, Hudson TJ, Owen RR, Owen RR, Thrush CR, Thrush CR, et al. A pilot study of barriers to medication adherence in schizophrenia. The Journal of clinical psychiatry. 2004;65(2):211-6.

36. Freudenreich O, Cather C, Evins AE, Henderson DC, Goff DC. Attitudes of schizophrenia outpatients toward psychiatric medications: relationship to clinical variables and insight. J Clin Psychiatry. 2004;65(10):1372-6.

37. Perkins DO. Predictors of noncompliance in patients with schizophrenia. The Journal of clinical psychiatry. 2002.

38. Karow A, Czekalla J, Dittmann RW, Schacht A, Wagner T, Lambert M, et al. Association of subjective well-being, symptoms, and side effects with compliance after 12 months of treatment in schizophrenia. The Journal of clinical psychiatry. 2007;68(1):75-80.

39. Cigarette Smoking in the United States [internet]. Tips from Fromer Smokers. [Available from:

http://www.cdc.gov/tobacco/campaign/tips/resources/data/cigarette-smoking-in-united-states.html.

40. Dalack G, Healy D, Meador-Woodruff J. Nictoine Dependence in Schizophrenia: Clinical Phenomena and Labratory Findings. AMm J Psychiatry. 1998;23(2):247-54

.

41. Lasser K, Boyd JW, Woolhandler S, Himmelstein DU, McCormick D, Bor DH. Smoking and Mental Illness. JAMA. 2000;284(20):2606.

42. Tandon R, Gaebel W, Barch DM, Bustillo J, Gur RE, Heckers S, et al. Definition and description of schizophrenia in the DSM-5. Schizophr Res. 2013;150(1):3-10.

43. Villalta-Gil V, Vilaplana M, Ochoa S, Haro JM, Dolz M, Usall J, et al. Neurocognitive performance and negative symptoms: are they equal in explaining disability in schizophrenia outpatients? Schizophr Res. 2006;87(1-3):246-53.

44. Howland RH. Now Take a Deep Breath: Inhaled Loxapine for the Treatment of Acute Agitation. Journal of Psychosocial Nursing and Mental Health Services. 2012;50(1):16.

45. Lesem MD, Tran-Johnson TK, Riesenberg RA, Feifel D, Allen MH, Fishman R, et al. Rapid acute treatment of agitation in individuals with schizophrenia: multicentre, randomised, placebo-controlled study of inhaled loxapine. Br J Psychiatry. 2011;198(1):51-8.

46. Noymer P, Myers D, Glazer M, Fishman RS, Cassella JV. The Staccato system: inhaler design characteristics for rapid treatment of CNS disorders. Respiratory Drug Delivery: Respiratory Drug Delivery; 2010.

47. FDA H. Label for Risperdal. 2009:1-99.

48. Labiris NR, Dolovich MB. Pulmonary drug delivery. Part I: Physiological factors affecting therapeutic effectiveness of aerosolized medications. British Journal of Clinical Pharmacology. 2003;56(6):588-99.

49. Laube BL, Laube BL. The expanding role of aerosols in systemic drug delivery, gene therapy, and vaccination. Respiratory care. 2005;50(9):1161-74.

50. Traini D. Inhalation Drug Delivery: Techniques and Products. First ed: Inhalation drug delivery Techniques and Products; 2013. p. 1-14.

51. Patton JS, Fishburn CS, Weers JG. The lungs as a portal of entry for systemic drug delivery. Proceedings of the American Thoracic Society. 2004;1(4):338-44.

52. Byron PR, Patton JS. Drug delivery via the respiratory tract. Journal of aerosol medicine. 1994;7(1):49-75.

53. Franck C, Budlovsky T, Windle SB, Filion KB, Eisenberg MJ. Electronic cigarettes in North America: history, use, and implications for smoking cessation. Circulation. 2014;129(19):1945-52.

54. Polosa R, Caponnetto P, Morjaria JB, Papale G, Campagna D, Russo C. Effect of an electronic nicotine delivery device (e-Cigarette) on smoking reduction and cessation: a prospective 6-month pilot study. BMC Public Health. 2011;11:786.

55. Caponnetto P, Caponnetto P, Auditore R, Auditore R, Russo C, Russo C, et al. Impact of an electronic cigarette on smoking reduction and cessation in schizophrenic smokers: a prospective 12-month pilot study. International journal of …. 2013;10(2):446-61.

56. Caponnetto P, Auditore R, Russo C, Cappello GC, Polosa R. Impact of an electronic cigarette on smoking reduction and cessation in schizophrenic smokers: a prospective 12-month pilot study. Int J Environ Res Public Health. 2013;10(2):446-61.

57. Leysen JE, Gommeren W, Eens A, De Courcelles DDC, Stoof JC, Janssen PA. Biochemical profile of risperidone, a new antipsychotic. Journal of Pharmacology and Experimental Therapeutics. 2006;247(2):661-70.

58. Claus A, Bollen J, De Cuyper H, Cuyper H, Eneman M, Malfroid M, et al. Risperidone versus haloperidol in the treatment of chronic schizophrenic inpatients: a multicentre double-blind comparative study. Acta Psychiatrica Scandinavica. 1992;85(4):295-305.

59. Kozielska M, Johnson M, Pilla Reddy V, Vermeulen A, Li C, Grimwood S, et al. Pharmacokinetic-pharmacodynamic modeling of the D(2) and 5-HT (2A) receptor occupancy of risperidone and paliperidone in rats. Pharm Res. 2012;29(7):1932-48.

60. Huang ML, Peer AV, Van Peer A, Woestenborghs R, De Coster R, Heykants J, et al. Pharmacokinetics of the novel antipsychotic agent risperidone and the prolactin response in healthy subjects. Clinical …. 1993;54(3):257-68.

61. Mannens G, Huang ML, Meuldermans W, Hendrickx J, Woestenborghs R, Heykants J. Absorption, metabolism, and excretion of risperidone in humans. Drug metabolism and disposition. 1993;21(6):1134-41.

62. Huang ML, Van Peer A, Woestenborghs R, De Coster R, Heykants J, Jansen AA, et al. Pharmacokinetics of the novel antipsychotic agent risperidone and the prolactin response in healthy subjects. Clin Pharmacol Ther. 1993;54(3):257-68.

63. Gibaldi M, Perrier D. Pharmacokinetics Second Edition Revised and Expanded: Marcel Dekker, Inc; 1982.

64. Gibaldi M, Koup JR. Pharmacokinetic concepts - Drug binding, apparent volume of distribution and clearance. European Journal of Clinical Pharmacology. 1981;20(4):299-305.

65. Zhou ZL, Li X, Peng HY, Yu XY, Yang M, Su FL, et al. Multiple dose pharmacokinetics of risperidone and 9-hydroxyrisperidone in Chinese female patients with schizophrenia. Acta Pharmacol Sin. 2006;27(3):381-6.

66. Olsen CK, Brennum LT, Kreilgaard M. Using pharmacokinetic-pharmacodynamic modelling as a tool for prediction of therapeutic effective plasma levels of antipsychotics. Eur J Pharmacol. 2008;584(2-3):318-27.

67. Nyberg S, Eriksson B, Oxenstierna G, Halldin C, Farde L. Suggested minimal effective dose of risperidone based on PET-measured D2 and 5-HT2A receptor occupancy in schizophrenic patients. Am J Psychiatry. 1999;156(6):869-75.

68. Nyberg S, Farde L, Eriksson L, Halldin C, Eriksson B. 5-HT2 and D2 dopamine receptor occupancy in the living human brain. Psychopharmacology (Berl). 1993;110(3):265-72.

69. Nyberg S, Eriksson B, Oxenstierna G, Halldin C, Farde L. Suggested minimal effective dose of risperidone based on PET-measured D2 and 5-HT2A receptor occupancy in schizophrenic patients. American Journal of Psychiatry. 1999;156(6):869-75.

70. Ikai S, Remington G, Suzuki T, Takeuchi H, Tsuboi T, Den R, et al. A cross-sectional study of plasma risperidone levels with risperidone long-acting injectable: implications for dopamine D2 receptor occupancy during maintenance treatment in schizophrenia. J Clin Psychiatry. 2012;73(8):1147-52.

71. Gear CW, Petzold LR. ODE methods for the solution of differential/algebraic systems. SIAM Journal on Numerical Analysis. 1984.

72. Patton JS, Brain JD, Davies LA, Fiegel J, Gumbleton M, Kim KJ, et al. The particle has landed--characterizing the fate of inhaled pharmaceuticals. J Aerosol Med Pulm Drug Deliv. 2010;23 Suppl 2:S71-87.

73. Sarasija S, Patil JS. Pulmonary drug delivery strategies: A concise, systematic review. Lung India. 2012;29(1):44-9.

74. Möller HJ. Risperidone: a review. 2005.

75. Amidon GL, Lennernäs H, Shah VP, Crison JR. A theoretical basis for a biopharmaceutic drug classification: the correlation of in vitro drug product dissolution and in vivo bioavailability. Pharmaceutical research. 1995;12(3):413-20.

76. Vasagam GA, Vasagam GA, Smith AA, Smith AA, Nawas CH, Nawas C, et al. Development of analytical method for Risperidone by UV Spectrophotometry using methanol as a solvent. Der Pharma …. 2010.

77. Soliman KA, Ibrahim HK, Ghorab MM. Formulation of Risperidone as Self-Nanoemulsifying Drug Delivery System in Form of Effervescent Tablets. Journal of Dispersion Science and Technology. 2012;33(8):1127-33.

78. Strickley RG, Strickley RG. Solubilizing excipients in oral and injectable formulations. Pharmaceutical research. 2004;21(2):201-30.

79. Sattanathan P, Babu JM, Vyas K, Reddy RB, Rajan ST, Sudhakar P. Structural studies of impurities of risperidone by hyphenated techniques. J Pharm Biomed Anal. 2006;40(3):598-604.

80. Suthar AP, Dubey SA, Patel SR, Shah AM. Determination of Risperidone and forced degradation behavior by HPLC in tablet dosage form. International Journal of PharmTech Research. 2009;1(3):568-74.

81. Dedania ZR, Dedania RR, Sheth NR, Patel JB, Patel B. Stability indicating HPLC determination of risperidone in bulk drug and pharmaceutical formulations. Int J Anal Chem. 2011;2011:124917.

82. Kumar MS, Kumar MS, Smith AA, Smith AA, Vasagam GA, Vasagam GA, et al. Development of analytical method for risperidone by UV spectrophotometry. International journal of …. 2010.

83. Kumar M, Pathak K, Misra A. Formulation and characterization of nanoemulsion-based drug delivery system of risperidone. Drug Dev Ind Pharm. 2009;35(4):387-95.

84. Kumar M, Misra A, Babbar AK, Mishra AK, Mishra P, Pathak K. Intranasal nanoemulsion based brain targeting drug delivery system of risperidone. Int J Pharm. 2008;358(1-2):285-91.

85. Deepakumari H, Mallegowda S, Vinay K, Revanasiddappa H. Simple and extraction-free spectrophotometric methods for risperidone in pure form and in dosage forms. Chemical Industry and Chemical Engineering Quarterly. 2013;19(1):121-8.

86. He H, Richardson JS. A pharmacological, pharmacokinetic and clinical overview of risperidone, a new antipsychotic that blocks serotonin 5-HT2 and dopamine D2 receptors. Int Clin Psychopharmacol. 1995;10(1):19-30.

87. Copley M. Understanding cascade impaction and its importance for inhaler testing. Copley Scientific.

88. Lewis D, Copley M. Inhaled Product Characterization. Particle Characterization. 2012:1-5.

89. O'Callaghan C, Barry PW. The science of nebulised drug delivery. Thorax. 1997;52 Suppl 2:S31-44.

90. Hess DR. Nebulizers: principles and performance. Respir Care. 2000;45(6):609-22.

91. Cipolla D, Gonda I, Shire SJ. Characterization of aerosols of human recombinant deoxyribonuclease I (rhDNase) generated by jet nebulizers. Pharmaceutical research. 1994;11(4):491-8.

92. Capasso RM, Lineberry TW, Bostwick JM, Decker PA, St Sauver J. Mortality in schizophrenia and schizoaffective disorder: an Olmsted County, Minnesota cohort: 1950-2005. Schizophr Res. 2008;98(1-3):287-94.

93. Klosterkotter J, Schultze-Lutter F, Ruhrmann S. Kraepelin and psychotic prodromal conditions. Eur Arch Psychiatry Clin Neurosci. 2008;258 Suppl 2:74-84.